Beyond the Knee Point: A Practical Guide to CT Saturation

Ariana Hargrave, Michael J. Thompson, and Brad Heilman
Schweitzer Engineering Laboratories, Inc.

This paper was presented at the 71st Annual Conference for Protective Relay Engineers and can be accessed at: https://doi.org/10.1109/CPRE.2018.8349779.

For the complete history of this paper, refer to the next page.

Revised edition released May 2020

Previously presented at the
PowerTest Conference, March 2019,
54th Annual Minnesota Power Systems Conference, November 2018,
72nd Annual Georgia Tech Protective Relaying Conference, May 2018,
and 71st Annual Conference for Protective Relay Engineers, March 2018

Previous revised editions released April 2019 and December 2018

Originally presented at the
44th Annual Western Protective Relay Conference, October 2017

Beyond the Knee Point: A Practical Guide to CT Saturation

Ariana Hargrave, Michael J. Thompson, and Brad Heilman, *Schweitzer Engineering Laboratories, Inc.*

***Abstract*—Current transformer (CT) saturation, while a fairly common occurrence in protection systems, is not often clearly understood by protective relay engineers. This paper forgoes the usual physics equations to describe how CTs saturate in a simple and intuitive way. We explain the differences between symmetrical and asymmetrical saturation and how remanence accumulates in the core of a CT. We then describe the CT equivalent circuit and how it results in the familiar CT excitation graph. ANSI ratings of CTs are explained, and we show how to analyze the performance of CTs using simple equations and tools. Finally, we explain how CT saturation can affect relay operation and show how to detect CT saturation in protective relay event reports. Real-world event reports are presented where correct relay operation was compromised as a result of incorrect current values from saturated CTs.**

I. Introduction

Current transformer (CT) saturation is not a new topic, and there have been many papers, books, application guides, and tutorials written on the subject. Sorting through this vast array of information to piece together a complete understanding of the topic is a time-consuming task and may not be realistic with the schedules and demands placed on many practicing engineers. Because of this, engineers' level of understanding is often limited to the familiar CT excitation graph. The following is a list of common questions related to CT saturation:

- Why does a CT saturate (Section II, Subsection B)?
- What is remanence, and do I have to worry about it (Section II, Subsection C)?
- What does it mean when a CT is a C800 (Section II, Subsection F)?
- I have a C800 multiratio CT tapped at 400/5. Is it still a C800 (Section II, Subsection F)?
- How do I make sure my CT will not saturate for my worst-case fault current (Section III)?
- The knee point determines the saturation voltage of a CT, right (Section II, Subsection E)?
- Will saturated CTs cause my relay to misoperate? What if they just saturate a little bit (Section V)?
- After a misoperation, how do I know if CT saturation was a cause (Section IV)?
- Can modern relays prevent misoperations due to CT saturation (Section VI)?

The goal of this paper is to explain CT saturation to the protective relay engineer and to answer these questions in a clear and practical way. As this paper demonstrates, a proper understanding of CT saturation must extend beyond the knee point.

II. CT Saturation Theory

To understand CT saturation, it is very important to understand the basic concept of how CTs work and what is actually happening when they saturate. This section describes what happens in the core of a CT during symmetrical saturation, asymmetrical saturation, and remanence. It then explains how this core activity corresponds to the CT equivalent circuit, ANSI voltage ratings, and the familiar CT excitation graph.

A. How CTs Work

In its simplest form, a CT consists of two sets of wire windings around an iron core, as shown in Fig. 1. The concept is the same for a window or bushing CT, which consists of a secondary winding around a core, with the primary winding being the primary conductor that passes through it. Transformers work based on the principle of electromagnetic induction. This principle states that an alternating magnetic flux in the presence of a loop of wire induces a voltage across that loop. Magnetic flux is simply the amount of magnetic field passing through a material such as a transformer core.

When alternating current I_P flows in the primary winding of a transformer, it generates an alternating magnetic field H, which corresponds to an alternating magnetic flux Φ, around the transformer core. This alternating magnetic flux passes through the secondary winding. What happens next depends on the load connected to the secondary winding.

If the secondary is connected to a burden, the alternating magnetic flux in the core induces an alternating voltage V_S across the secondary winding. This causes a corresponding alternating current I_S to flow in the secondary winding. The alternating current in the secondary creates its own alternating magnetic field and alternating magnetic flux that oppose those created by the primary winding. These primary and secondary fluxes cancel, leaving a negligible amount of net flux in the core. This occurs until the core becomes saturated.

If the secondary is open-circuited, the alternating magnetic flux in the core induces a very high alternating voltage V_S across the secondary winding. V_S remains on the terminals with no secondary current flowing, which is why it is very dangerous to open-circuit an in-service CT. Because I_S cannot flow, it cannot create an opposing magnetic field, leaving a net flux in the core equal to the flux created by the primary current.

This magnetic behavior is modeled when we introduce the CT equivalent circuit in Section II, Subsection D. For now, know that the induction of voltage V_S is a result of the magnetic field created by I_P along with the internal impedances of the transformer and the connected load. For simplification going forward, we assume a fixed linear burden is connected to the CT. When this is the case, Ohm's law mandates that the secondary current in the CT and the voltage across the magnetizing impedance are directly proportional.

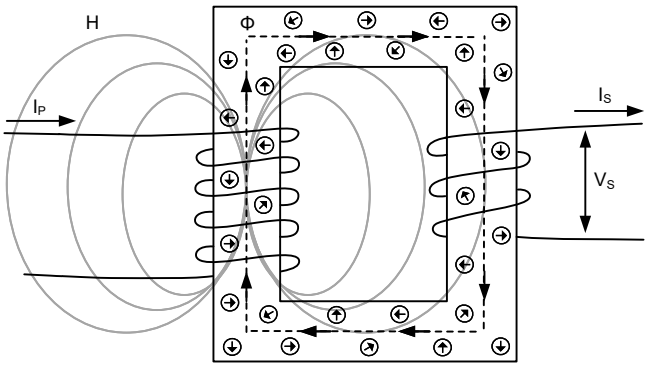

Fig. 1. CT drawing

B. Why Does a CT Saturate?

In an ideal world, the secondary current leaving the CT (I_S) is an exact replica of the primary current (I_P) divided by the ratio of the number of turns in each winding (CT ratio). However, when a CT saturates, I_S does not accurately replicate I_P. The reason a CT saturates is related to what physically occurs inside a CT during the electromagnetic induction process. The iron core of a CT is made up of a fixed number of magnetic dipoles, which can be thought of as molecular magnets. Ideally, these magnets are randomly arranged in polarity throughout the core, as shown in Fig. 1.

When alternating current (I_P) flows in the primary winding and generates the magnetic field (H), the strength of this magnetic field affects the magnets in the core and causes them to start lining up (in the same direction as the magnetic field) to produce the magnetic flux (Φ). The more current I_P that flows, the stronger the magnetic field (H) becomes, and the more magnets become lined up. The number of magnets that are lined up at a given time is the flux density (B). When all the magnets in the core are aligned in the same direction, the maximum flux density of the core is reached and the CT core is said to be saturated.

The relationship between the magnetic field strength (H) and the magnetic flux density (B) is given by the B-H curve of the core, as shown in the example in Fig. 2. Different types of core materials have different B-H curves, which depend on the ability of the material to support a magnetic field.

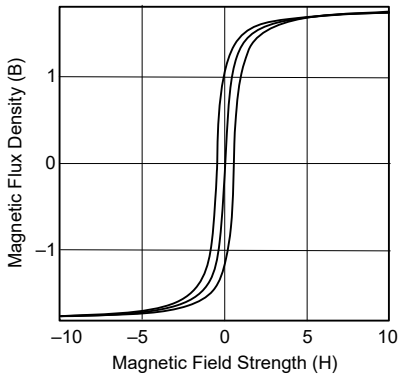

Fig. 2. Example B-H curve

How this magnetic behavior affects the ability of the CT to reproduce current is simple: it is the change in flux caused by the magnets changing direction that induces voltage V_S across the secondary winding of the CT. Voltage V_S, in turn, generates current I_S through the connected circuit. When the core reaches maximum flux density, it is fully saturated and there are no more magnets remaining to change direction. This causes voltage V_S to drop to zero, and current I_S ceases to flow.

CT saturation can occur in two forms: symmetrical saturation and asymmetrical saturation. These saturation types are explained in the following subsections. For a detailed explanation of the mathematics of CT saturation, see [1].

1) Symmetrical Saturation

Symmetrical saturation is the result of a symmetrical primary current being applied to the CT that is too large for the CT core to handle for a given burden.

Fig. 3 shows an example of the primary current (I_P) and secondary current (I_S) of a CT during symmetrical saturation. Ideally, before the current is applied at Point *a*, the magnets in the core are aligned in random directions (no remanence, which is discussed later in this paper). Between Points *a* and *b*, as I_P starts to flow in the first positive half cycle, the magnets start to line up in the positive direction. Because there is a change in flux during this time, the current I_S matches I_P exactly (assuming a CT ratio of 1:1). Before the positive half cycle is over, at Point *b*, all of the magnets available in the core are lined up in the positive direction, and the core has reached maximum flux density (saturation). At this point, even though I_P continues to flow, there is no more change in flux, V_S drops to zero, and I_S drops to zero. I_S stays at zero until I_P begins to flow in the negative direction, reversing the magnetic field. This negative flow, beginning at Point *c*, causes the magnets to begin aligning in the negative direction. This changing flux allows the generation of voltage V_S and allows I_S to follow I_P again until all of the magnets are aligned in the negative direction at Point *d*. Because maximum flux density (saturation) has been reached again, V_S and I_S again drop to zero.

The example in Fig. 3 shows the primary current decreasing in magnitude every cycle. The point of this is to show that if primary current magnitude decreases, the CT is saturated for less time. The lower magnitude in the second cycle of Fig. 3 generates a weaker magnetic field, requiring less flux density to replicate the current correctly. Because fewer magnets are used, I_S reliably replicates I_P for a longer time until all the magnets are aligned. In the third cycle, the magnitude of I_P has been lowered to the point that the CT does not saturate and replicates current correctly the entire time.

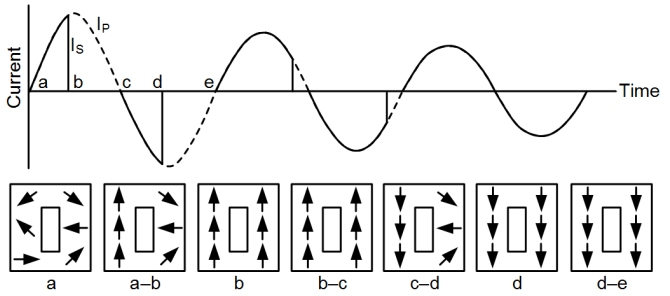

Fig. 3. Primary currents, secondary currents, and magnetic dipoles in the core during symmetrical saturation

2) Asymmetrical Saturation

The other form of saturation, asymmetrical saturation, results from high levels of dc offset in the primary sinusoidal current being applied to the CT. The current peaks are not symmetrical around zero. DC offset is when there is more area under the curve above the zero crossing than there is below the zero crossing (or vice versa). Fig. 4 shows how a waveform with high dc offset can cause a CT to quickly saturate. From Points *a* to *b*, magnets are all lining up in the positive direction and the CT has not saturated. When I_P becomes negative, from Points *b* to *c*, magnets start changing directions and lining up in the negative direction. Because there is such a small amount of area under the curve between Points *b* and *c*, not very many of the magnets have lined up in the negative direction when the I_P current goes back above the zero crossing (Point *c*) and they are forced to start lining up in the positive direction again. Finally, at Point *d*, all of the available magnets are lined up in the positive direction and the core saturates. The dc offset—not the magnitude of the fault current itself—is what causes the saturation. The fact that I_P is not below the zero crossing long enough to reset the magnets in the opposite direction is what causes saturation to occur. Notice that the amount of time the CT is saturated is less with each cycle as the dc component decays.

The magnetic behavior described previously is referred to in [1] as the integration of the volt-time integral. Recall that with a fixed burden, current is directly proportional to voltage. The amount of flux that accumulates in the core of a CT is directly proportional to the area under the voltage (or current) curve. A given CT can handle some maximum amount of flux before it saturates. This limit is defined by a symmetrical sine wave with a fixed voltage magnitude and fixed area under the curve in both the positive and negative directions. As long as the actual CT waveform does not exceed this positive or negative volt-time area, the CT will not saturate. Consider the dc offset of the asymmetrical current in Fig. 4. This dc offset will result in an accumulating positive volt-time area that eventually reaches the maximum that the CT can handle at Point *d*, where saturation occurs.

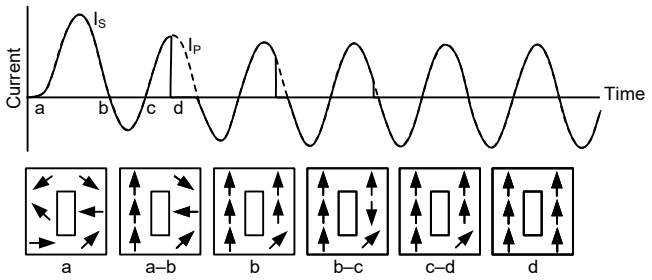

Fig. 4. Primary currents, secondary currents, and magnetic dipoles in the core during asymmetrical saturation

The time it takes for a CT to saturate can vary depending on current magnitude, dc offset, X over R ratio, burden, and remanence. An equation to calculate the time it takes a CT to saturate is found in [2]. Symmetrical saturation normally occurs within the first half cycle after fault inception, whereas asymmetrical saturation can take several cycles to occur. Because the magnitude of the current does not need to be as high for asymmetrical saturation to occur, it usually takes longer for the flux density to reach its maximum.

Not all saturated waveforms are as obvious to the eye as the waveform in Fig. 3, which has sharp edges and large chunks missing. With low levels of saturation, a saturated waveform can be hard to detect. Fig. 5 shows waveforms from CTs with light, medium, and heavy levels of symmetrical saturation [3].

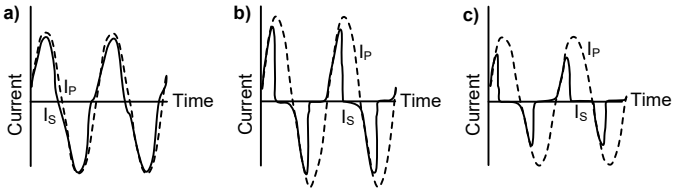

Fig. 5. Varying degrees of CT saturation: light saturation (a), medium saturation (b), and heavy saturation (c)

The waveshape of secondary current I_S during saturation also depends on the type of load connected. Fig. 6 shows the waveshape with a purely resistive burden compared with a burden that has both resistive and reactive components of similar magnitudes. The difference in waveshape is because of the fact that current through an inductive load cannot change instantaneously, so it takes some time for the current to decay.

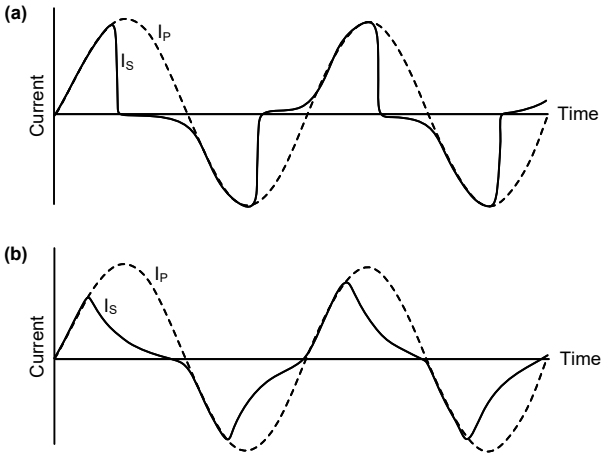

Fig. 6. Saturated waveshapes for resistive (a) and resistive-inductive (b) loads

C. Remanence

If a CT has reached saturation and a switch is opened to remove the primary current, we would expect the magnetic field (H) to disappear and the flux density (B) to reduce to zero. However, flux density does not go to zero when the primary current stops flowing. When primary current is removed, the magnetic field that causes the magnets to change orientation disappears, and the magnets in the core remain in their present orientation. The magnets will not move again until exposed to another magnetic field. The amount of flux density remaining in the core is called remanence. The fact that the magnets still point in the direction they were in when the magnetic field was removed gives the core "memory" (like a permanent magnet). This remanence remains in the core until primary current is reapplied. If the reapplied current is opposite in polarity from the original, flux density is created in the opposite direction of the prior remanence.

The example of a switch being opened to remove primary current is exactly what happens when a relay trips a circuit breaker during a fault. Recall that when a breaker operates, current is interrupted at a zero crossing. In Section II, Subsection B, we show that for both symmetrical and asymmetrical currents, there is a positive or negative flux density in the core when the current zero crossing occurs. This flux density can be significant during high-magnitude asymmetrical current (when a dc transient is present). This remanence remains in the CTs after the breaker opens and affects their behavior the next time they are energized. Remanence can either help or hinder a CT's performance, depending on whether the remanence is of the same polarity or opposite polarity of the next current that the CT measures. It takes more time for the CT to saturate if the remanence is the opposite polarity of the current and less time if it is the same polarity.

Examination of the example B-H curve in Fig. 2 shows another factor that causes the magnetic core to have remanence. Note that the curve follows a loop trajectory. The flux density (B) lags the field intensity (H) as it goes through a power system cycle. This phenomenon is called hysteresis.

The only way to remove this remanence is by degaussing the CT. Degaussing can be done by applying primary rated current and a variable load to the CT secondary terminals. Start the load at a high resistance to cause the CT to saturate in both the positive and negative directions. Then bring the CT out of saturation by slowly reducing the load (and thus the secondary voltage) to zero. The only convenient time to do this is during system maintenance, but in practice it is almost never done. Annex C of [2] shows that in a survey of 141 CTs on a 230 kV system, 43 percent had more than 40 percent remanence when measured.

The effect of remanence on CT saturation is shown in Fig. 7. In this example, the CT is sized to perfectly handle an ac current signal of a certain magnitude without saturating. In addition, there is some remanence left over in the core of the CT. Before the current is applied, between Points *a* and *b*, some of the magnets in the core are already aligned in the positive direction because of remanence. Between Points *b* and *c*, as I_P starts to flow in the first positive half cycle, the remaining magnets also line up in the positive direction. Because there is a change in flux during this time, the current I_S matches I_P divided by the turns ratio. Before the positive half cycle is over, at Point *c*, all the magnets available in the core are lined up in the positive direction and the core has reached saturation. At this point, even though I_P continues to flow, there is no more change in flux and V_S and I_S drop to zero. I_S stays at zero until I_P begins to flow in the negative direction, reversing the magnetic field and allowing flux to accumulate in the opposite direction. This occurs at Point *d*, where magnets begin to align in the negative direction and the changing flux allows I_S to follow I_P again. By the time I_P reaches its negative peak at Point *e*, only half of the maximum core flux is aligned in the negative direction. This allows I_S to continue to follow I_P until all the magnets are aligned in the negative direction, at Point *f*. Although we have reached maximum flux density again, this is where I_P changes direction and we start accumulating flux in the positive direction.

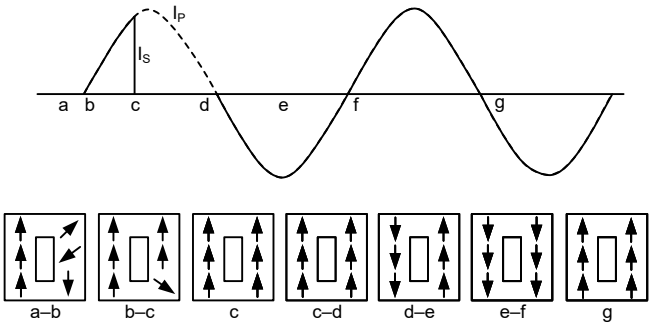

Fig. 7. Primary currents, secondary currents, and magnetic dipoles in the core with remanence

As we can see from this example, saturation as a result of remanence is short-lived, lasting about half a cycle. Because of this short saturation time, remanence has little effect on standard protection algorithms and is normally neglected in CT saturation calculations [4] [5]. Any relaying algorithm that performs faster than this should include some level of built-in protection against CT saturation.

D. CT Equivalent Circuit

We can represent the behavior of the C-class CT shown in Fig. 8a with the simplified equivalent circuit shown in Fig. 8b.

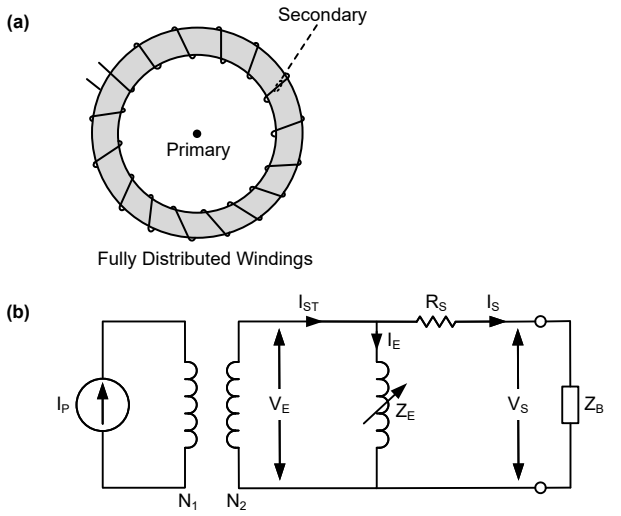

Fig. 8. Class C CT (a) and Simplified CT equivalent circuit (b)

I_P (the primary current), V_S (the secondary CT terminal voltage), and I_S (the secondary load current) are self-explanatory. N_1 and N_2 represent the turns ratio of the CT, and the ratio current I_{ST} is the primary current divided by this ratio. The circuit connected to the secondary of the CT is the burden represented by Z_B and includes the impedance of the relay and CT leads. The resistance R_S represents the secondary winding resistance of the CT. The magnetizing behavior of the core of the CT is represented by a varying reactance, Z_E. This impedance changes as the CT saturates, resulting in varying secondary excitation voltage V_E and varying exciting branch current I_E. (Although Z_E technically has a real and reactive component, most practical CT analysis is close enough when neglecting the angles of the impedances.)

In the CT equivalent circuit in Fig. 8, the constant current source I_P drives the total secondary current I_{ST} as determined by the turns ratio. I_{ST} is the current that is measured by the load if the CT is ideal. However, we must take into account the magnetizing behavior of the CT core that is represented by the varying impedance Z_E. Because magnetization is nonlinear, different values of impedance (Z_E) must be used for different states of operation (normal conditions vs. saturated conditions).

We can think of Z_E as a varying impedance that changes with flux density. It has a very high value under normal conditions and a very low value (basically a short-circuit) when the CT is saturated. The excitation current (I_E) is the current that is lost through the magnetizing branch and corresponds to the CT error. We can also refer to this as "error current." I_E is small when the Z_E impedance is large (during normal conditions) and large when the Z_E impedance is small (during saturation). The current measured by the load (I_S) is what is left of the ratio current (I_{ST}) after the error current (I_E) is lost through the magnetizing impedance (Z_E). Therefore, the current the relay sees is accurate during times of high Z_E impedance (low error current), and it is much lower than expected during times of low Z_E impedance (high error current). This behavior gives us the classic saturation waveform shown in Fig. 3.

Fig. 9, adapted from [6], explains the saturation process in the time domain. The graph in Quadrant III shows the primary current I_P being applied to the CT. The graph in Quadrant II shows the flux density over time. At time t_0, when the CT is first energized, the flux density starts to increase from whatever remanent value was left in the CT at the last de-energization. Flux density continues to rise in the CT during the positive half cycle and decreases during the negative half cycle. Time t_3 is the point of maximum flux density, when the CT is fully saturated. The graph in Quadrant IV shows the excitation (error) current over time. We can see that the highest excitation current occurs at the point of maximum flux density. The graph in Quadrant I shows flux density versus excitation current and is made up of the intersection of points between the graph in Quadrant II and the graph in Quadrant IV. The graph in Quadrant I is not time-dependent, but simply shows the amount of excitation current that is measured for a given flux density. This graph shows that when the flux density is low, the excitation (error) current is low (because Z_E is a high value). As flux density increases and the CT approaches saturation, the excitation current increases substantially (because Z_E is a lower value), meaning less current will be available to the burden. Notice that the graph in Quadrant I corresponds directly to the B-H curve in Fig. 2, where the excitation current I_E is proportional to the magnetic field strength H.

The flux density in Fig. 9 is directly proportional to both the flux and the excitation voltage V_E. We can therefore interpret the graph in Quadrant I as the instantaneous relationship between V_E and I_E, and use it to understand the changing impedance of the CT excitation branch (Z_E). The slope of the curve is the ratio of V_E/I_E, which Ohm's law allows us to characterize as Z_E. We can easily visualize that the curve is made up of two linear sections and that the knee point is where the two linear sections transition. The steep part of the curve, where the ratio of V_E/I_E is high (Z_E is high), represents where the core is not saturated. This is called the iron-core reactance region of the curve. The flat part of the curve, where the ratio of V_E/I_E is low (Z_E is low), represents where the core is saturated. This is called the air-core reactance region of the curve because the saturated iron core has no better permeability than air.

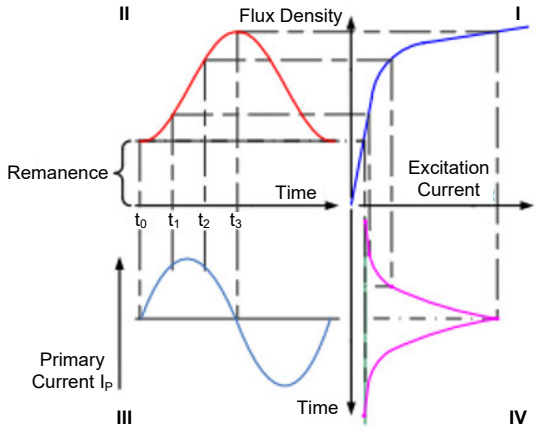

Fig. 9. Relationship between primary current, core flux density, and error current in a CT

E. Excitation Graph

Being able to interpret the classic knee-point (excitation) graph of a CT is an integral part of understanding CT saturation. The previous sections explain what happens as a CT saturates in the time domain and why CT saturation results in secondary waveforms like those in Fig. 5. However, it is sometimes helpful to think in terms of rms quantities instead of samples on a waveform over time. The excitation graph in Fig. 10 shows the relationship between the excitation voltage V_E and excitation (error) current I_E of a CT in rms quantities. In other words, the graph shows what we would read if we varied the magnitude of the ac current on the primary of the CT and were somehow able to measure the V_E voltage and I_E current with an rms meter. This graph shows the rms value of the entire waveform, not just a specific point in time when the CT is not saturated or fully saturated. The graph in Fig. 10 looks similar in shape to the graph in Quadrant I of Fig. 9, but Fig. 9 consists of instantaneous quantities and Fig. 10 consists of rms quantities. Another difference between Fig. 9 and Fig. 10 is a result of the equation $\Phi = B \bullet A$. Basically, the flux density (B) in Fig. 9 is multiplied by the area of the core (A) to get the magnetic flux (Φ), which is proportional to the excitation voltage (V_E).

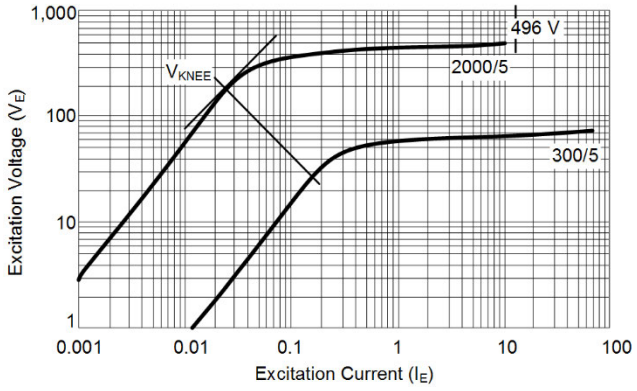

Fig. 10. Example excitation graph for a C400 CT [7]

Excitation graphs are developed from measurements at the factory. Graphs for multiratio CTs show multiple lines, one for each tap. Fig. 10 shows the highest and lowest taps of a C400, 2000/5 multiratio CT. The magnetizing impedance Z_E can be calculated at any point on the graph by dividing V_E by the corresponding value for I_E. This results in values for Z_E that vary nonlinearly. Recall again that the values on the excitation graph are all rms values. In reality, Z_E, V_E, and I_E change continually with every instantaneous value during a power system cycle.

A simple test can be performed to obtain the excitation graph of a CT. With the primary of the CT open, a user can apply a known voltage across the secondary terminals and measure the current flowing from the source into the CT. With voltage applied on the secondary side, the equivalent circuit of the CT changes. In this test, the voltage applied is V_E and the current measured is I_E. The user can then plot V_E versus I_E for various values of V_E.

Using the graph in Fig. 10 for the 2000/5 CT as well as the CT equivalent circuit in Fig. 8, we can analyze how the CT behaves during different operating conditions (normal vs. saturated). For simplicity, these examples neglect the CT secondary resistance R_S.

1) Normal Operation

The area of normal operation is along the high linear slope portion of the excitation graph, where I_E and V_E increase proportionally to each other. We select a random point on the line in this region as (I_E = 0.01 A, V_E = 60 V) and apply these values to our equivalent circuit, as shown in Fig. 11. We then solve for Z_E = 6,000 Ω, which is a very high impedance. If we connect a burden of 4 ohms, we can solve for I_S = 15 A and I_{ST} = 15.01 A. We see that because the error current is so small, the ratio current (I_{ST}) is very close to the current the load actually sees (I_S), meaning the CT is behaving properly.

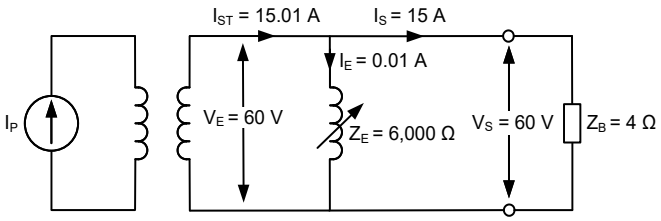

Fig. 11. Equivalent circuit example of normal operation

2) Saturation

The area of saturation is along the low linear slope portion of the excitation graph, where a small change in V_E results in a very large change in I_E. We select a random point on the line in this region as (I_E = 10 A, V_E = 496 V) and apply these values to the equivalent circuit, as shown in Fig. 12. We then solve for Z_E = 49.6 Ω, which is a very small impedance. If we connect a burden of 4 Ω, we can solve for I_S = 124 A and I_{ST} = 134 A. We see that because the error current is so large, the ratio current (I_{ST}) is not very close to the current the load actually sees (I_S), meaning the CT is behaving poorly.

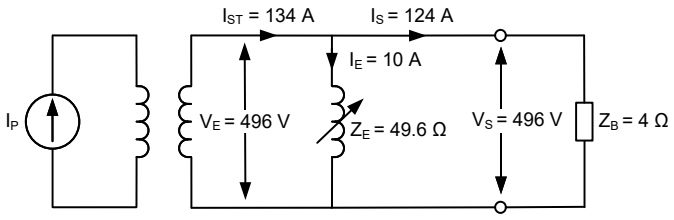

Fig. 12. Equivalent circuit example of saturation

The shape of this area of the excitation graph confirms what is happening magnetically when a CT saturates. Recall that V_E is generated by the magnetic field from the current flowing in the primary winding. In addition, recall from our time-domain analysis that during the parts of the waveform when the CT is saturated (high levels of V_E), the current is diverted away from the load and into the magnetizing branch. If this happens for a large percentage of the waveform, we can expect a higher rms current for I_E.

The 2000/5 CT in Fig. 10 has a maximum V_E of 496 V. This means that no matter how much primary current is coming into the CT, the resulting magnetic field can only produce a voltage as high as 496 V on the secondary winding. This voltage is limited by the amount of core material, and thus magnetic dipoles, available in the CT. A CT with a larger core is able to support a higher voltage and has a higher rating (discussed later in the paper). The actual voltage on the secondary terminals is 496 V minus the voltage drop across the secondary winding resistance R_S.

3) Definition of Saturation and Knee-Point Voltage

In previous sections of the paper that explain saturation in the time domain, we said that the CT was saturated during the sections of the waveform where the flux was not changing and the secondary current dropped to zero. This is an accurate definition of saturation in the time domain.

It is also important to define saturation in terms of rms quantities so we can work with the CT equivalent circuit and the CT excitation graph. IEEE does not define a specific saturation point, but does define the knee point of the excitation curve as the voltage at the point where a 45-degree line hits tangent to the curve. This is shown in Fig. 10 and results in a knee-point voltage of 200 V for the 2000/5 CT. The knee point of the graph defines where the CT starts to exhibit nonlinear behavior resulting from the beginning of core saturation. However, for rms analysis, it is not practical to define saturation at the point where it first begins. Instead, saturation typically refers to the point where the CT error starts to exceed 10 percent. This aligns with definitions of the ratio error and the terminal voltage rating in Section II, Subsection F. For now, understand that *the point of saturation is not the same as the knee-point voltage* (a very common misconception). The knee-point voltage is typically 46 percent of the saturation voltage [8].

F. CT Accuracy Class

CT accuracy is often discussed using the CT ratio error and terminal voltage rating.

1) Ratio Error

The accuracy of a CT is defined as the extent to which the current in the secondary circuit reproduces the current in the primary circuit in the proportion stated by the marked ratio [2]. There are two ways to measure the accuracy of a CT—a direct test or an indirect test. A direct test is done by injecting a known primary current into the CT and calculating the difference between the injected primary current and the measured secondary current at the terminals (after taking into account the marked ratio). Although this is the simplest and most accurate way to test CT accuracy, it is not practical for relaying CTs because the extremely high current magnitudes that are required to be injected into the primary to achieve 20 times nominal are difficult to generate.

An indirect test is described in [9] as follows, which is similar to the excitation test described in Section II, Subsection E. First, calculate the equivalent V_E for a desired secondary current I_S and total burden ($Z_B + R_S$). Next, with the primary open-circuited, inject this voltage between the secondary terminals of the CT and measure the excitation current I_E. Then use (1) to calculate the percent ratio error. We define saturation as the point when the CT ratio error exceeds 10 percent.

$$\text{Ratio error}\,(\%) = \frac{I_E}{I_S} \cdot 100 \tag{1}$$

At first glance, (1) might seem like an incorrect equation to calculate error. When we try to define how well a CT reproduces current, a standard error calculation would compare the actual secondary current coming out of the CT terminals (I_S) with the expected or ideal secondary current (I_{ST}). Instead, (1) compares the error current (I_E) with the actual secondary current (I_S). Appendix A explains where (1) comes from and relates it to the more intuitive definition of error.

2) Terminal Voltage Rating

Most protection CTs in the United States are ANSI Class C. To be classified as a Class C CT, the CT must be constructed so that it has negligible leakage flux. If the leakage flux can be neglected, the performance of the CT can be determined by calculation (Class C). That generally requires that the CT be constructed with a toroidal core with fully distributed windings and a single primary winding, as shown in Fig. 8. The generic CT shown in Fig. 1 would be considered a Class T because the leakage flux in a CT constructed like this cannot be neglected. Class T means that the performance of the CT can only be accurately determined by test.

The number following the *C* is the secondary terminal voltage rating. IEEE defines the secondary terminal voltage rating as "*the CT secondary voltage that the CT will deliver when it is connected to a standard secondary burden, at 20 times rated secondary current, without exceeding a 10% ratio error* [2]."

This is the highest V_S voltage the core will support without going into significant saturation and assumes steady-state, symmetrical (no dc offset) current. An increase in primary current that tries to force a voltage beyond this point simply results in more error current and a very small, disproportionate

increase in current delivered to the load. The definition also states that assuming a 5 A nominal CT, 100 A is delivered to a standard burden when V_S matches the voltage rating of the CT. IEEE defines standard burdens for relaying CTs as 1, 2, 4, and 8 Ω. Consequently, the standard voltage ratings for 5 A nominal relaying CTs are C100, C200, C400, and C800 (20 times the 5 A rated secondary current) [9]. For example, a C400 accuracy class on a 5 A CT means that the ratio error will not exceed 10 percent for any current up to 100 A secondary (20 times the rated current) as long as the burden does not exceed the 4 Ω standard burden.

From this definition, the voltage rating of a CT defines voltage V_S, burden Z_B, and current I_S in the example shown in Fig. 13 for a C400, 5 A nominal CT. The definition also tells us that at this voltage, the ratio error (I_E / I_S) is a maximum of 10 percent. If we assume this worst case, then I_E must equal 10 A. We can then back-calculate to find I_{ST} = 110 A, which is the primary current divided by the turns ratio. If we go above this, we will start getting more than 10 percent error on the output, and the current the connected load reads will not be reliable. Similarly, increasing the burden Z_B to a value greater than the standard burden will also result in an increased error. When applying CTs, a simple rule of thumb to avoid a symmetrical saturation error over 10 percent is to use a burden equal to or less than the standard burden and ensure that the worst-case secondary fault current is less than 100 A.

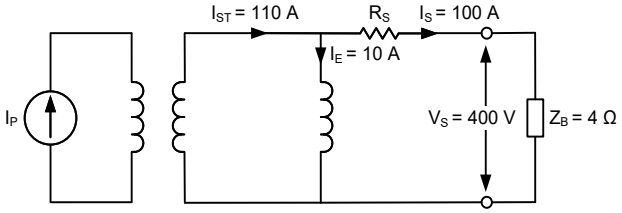

Fig. 13. Example for a C400, 5 A nominal CT

IEEE defines common CT voltage ratings as C100, C200, C400, and C800. Because the ratings are defined at specific voltage levels, not all CTs with the same voltage rating are created equal. For example, a CT with a terminal voltage of 810 V and a CT with a terminal voltage of 1,000 V would both be classified as C800. The CT with the excitation graph shown in Fig. 10 has an excitation voltage of 496 V at an error current of 10 A. To get the terminal voltage V_S, we subtract the voltage drop across the secondary winding resistance (R_S • 100 A) from the excitation voltage of 496 V. If the resulting terminal voltage is over 400 V, we classify the CT as a C400 CT [2].

It is important to note that these voltage ratings only apply to the full winding ratio of the CT, and tapping down a CT reduces its accuracy. Because both windings are distributed around the same core, they are each subject to the same flux and the voltage induced across every turn of any winding is the same. That is, the maximum volts per turn the CT can support without symmetrical saturation is fixed by the cross-sectional area of the core. If we choose to tap a CT at anything other than its full winding, there will be less voltage available at the terminals because not all of the available turns are connected to the load. In Fig. 10, for example, we can see that the 300/5 tap of the CT has a much lower terminal voltage at 10 A of error current than the full 2000/5 tap. For multiratio CTs, the voltage rating of a tap is directly proportional to the CT ratio corresponding to the tap divided by the full CT ratio (assuming the windings are fully distributed around the core). For example, if a C400, 1200/5 CT is operating on a 600/5 tap, the voltage rating at 600/5 is calculated as shown in (2).

$$V_{TAP} = C400 \bullet \left(\frac{600/5}{1200/5} \right) = C200 \tag{2}$$

This means that the CT supports a voltage of 200 V at 20 times rated secondary current of 100 A, which results in a standard burden of 2 Ω.

A final note on CT ratings and the knee point: notice that the knee point of the graph in Fig. 10 is V_E = 200, which is half of the ANSI voltage rating of the CT (C400). In fact, 400 V is not even on the high linear slope portion of the graph. Recall again that the knee point only shows where the CT behavior starts to become nonlinear, while the ANSI rating defines the point of 10 percent error. The ANSI rating, not the knee point, defines the practical threshold for saturation. Because the knee-point voltage is normally 46 percent of the saturation voltage, a popular rule of thumb to avoid saturation is to ensure that the ANSI rating is twice the terminal voltage developed by the maximum fault current [8]. This ensures operation near the knee point for the maximum symmetrical fault current.

III. Analyzing CT Performance

When a CT saturates, it provides distorted information to the connected relay, which can cause the relay to behave unexpectedly. When selecting a CT for a protective relay application, it is important to check if the CT saturates for the levels of fault current that will occur on the system. This section explains an equation that can be used to determine if a CT will saturate for given fault conditions.

A. CT Steady-State Performance Analysis

Equation (3) is the criterion to avoid CT saturation for symmetrical fault currents. Real-world faults are rarely symmetrical, so this equation should never be used practically to analyze CT performance. It is explained here and derived in Appendix B as a basis for the more practical equation in Section III, Subsection B. Equation (3) can be used to determine the maximum allowable fault current for a given burden or maximum allowable burden for a given fault current.

$$\frac{I_{FAULT}}{I_{PRI}} \bullet \frac{Z_B + R_S}{Z_{B\,STD} + R_S} \leq 20 \tag{3}$$

The terms in (3) are defined as follows:

I_{FAULT} is the maximum fault current in primary amperes for a given fault.

I_{PRI} is the primary current rating of the CT (e.g., for a 2000/5 CT, I_{PRI} is 2,000.)

Z_B is the actual burden of the CT's secondary circuit.

R_S is the internal resistance of the CT secondary winding.

$Z_{B\,STD}$ is the standard burden of the CT (e.g., for a C800 CT, the $Z_{B\,STD}$ is 8 Ω).

Z_B includes both the impedance of the connected relay and the impedance of the leads from the CT to the relay. Microprocessor-based relays have a negligible burden, but electromechanical relays do not. The impedance of the leads is determined by the wire gauge, the length of the leads, how the CTs are connected, and the fault type. #10 AWG copper wire has a resistance of 0.9989 Ω per 1,000 feet. Reference [10] shows how to calculate the resistance of other wire gauges. When using wye-connected CTs and performing the calculation for a single-phase-to-ground fault, a two-way lead burden should be used because the fault current has to make a full loop through the CT circuit (phase and neutral) and back to the relay. When using wye-connected CTs and performing the calculation for a three-phase fault, a one-way lead burden should be used because the fault current for a single phase sums with the other two phases at the neutral point of the wye connection and no current will flow through the neutral. This is derived in [5], which also shows how to calculate the burden when using delta-connected CTs.

R_S, the secondary winding resistance of the CT, is specified on the CT data sheet. The R_S value is directly related to the resistance of the wire and the number of turns and is therefore dependent on the tap for multiratio CTs.

$Z_{B\,STD}$ is the standard burden of the CT and must be adjusted if the CT is not tapped at its full ratio. In these instances, the standard burden must first be multiplied by the ratio of the tap rating to the full rating. For example, for a C800, 2000/5 CT tapped at 1200/5, the standard burden is shown in (4). The resulting C-rating for the tap would be 4.8 • 100 A = C480.

$$Z_{B\,STD} = \frac{800}{20 \bullet 5} \bullet \frac{1,200}{2,000} = 4.8 \tag{4}$$

B. CT Transient Performance Analysis

Section II shows that symmetrical fault currents are not the only risk for CT saturation. Fault currents with an exponentially decaying dc offset, caused by the X/R ratio of the system, can produce significant CT saturation. Selecting CTs based only on symmetrical fault current is not advised because it ignores the risk of heavy CT saturation when the fault current includes dc offset.

To account for dc offset, we can improve (3) by including an extra X/R term, resulting in (5) [5]. This extra term is the X/R ratio of the entire Thevenin equivalent of the system, from the source to the fault, through the particular CT. Equation (5) only considers dc offset from sinusoidal fault current, not offset from nonsinusoidal sources like transformer inrush. Appendix C gives an example of using (5) to analyze asymmetrical saturation in a CT.

$$\frac{I_{FAULT}}{I_{PRI}} \bullet \frac{Z_B + R_S}{Z_{B\,STD} + R_S}\left(\frac{X}{R} + 1\right) \le 20 \tag{5}$$

The initial magnitude of the dc offset that occurs is determined by the fault incidence angle, and the time it takes for the dc offset to decay is determined by the X/R ratio of the system. Equation (5) is quite conservative and assumes a worst-case, completely offset waveform, which is not often the case in the real world. Any fault other than the worst case will result in less saturation. Therefore, a value over 20 in this equation does not mean that the CT *will* saturate for that fault current—just that it *could*, assuming the fault current had the worst-case dc offset.

C. What About Remanence?

There is no way to predict the value of remanence that may exist in a CT at a given instant in time. As described in Section II, remanence can either impair or improve the CT behavior for a given fault. The worst case is when a fault produces flux of the same sign as the remanence. In this case, the flux change required to saturate the CT equals the difference between the core saturation flux and the remanence.

Regardless of how much remanence exists in a CT, recall from Section II that the effect remanence has on saturation only lasts about half a cycle. Modifications to (5) have been made to account for the effects of remanence by derating the CT, but they are only valid for the first half cycle of the fault [2]. Using these modifications to size CTs is unnecessarily conservative and often yields impractically large CTs. Be aware that because of the random nature of remanence, even a CT that was properly sized using (5) may still saturate momentarily. This saturation will be short-lived and should have little effect on the performance of standard relay algorithms.

Despite the best intentions, there are certain times when the use of (5) to select CTs that will never saturate becomes an exercise in futility. One such example is on applications near a generator bus. Here, the X/R ratios and fault current magnitudes are extremely high, and it is usually impossible to avoid asymmetrical saturation even with the largest CTs. Reference [2] recommends selecting the highest practical rating for the CTs and always matching the CTs on the terminal and neutral sides of the generator to each other (same ANSI voltage rating, CT ratio, and connected burden). This way, even though we know the CTs will saturate, they will saturate in the same way and the saturated waveforms will cancel each other out in the differential calculation. Because not all CTs with the same voltage rating are created equal, it is important to make sure that both CTs have the same excitation curve, knee-point voltage, and terminal voltage at 10 A of excitation current. See Section III, Subsection D for an example illustrating this point.

Another example of not being able to avoid saturation is in low- and medium-voltage switchgear applications, where fault currents are high and space requirements force the use of small and poorly-rated CTs. Refer to [11] and [12] for selection criteria for low-voltage applications. For more information on selecting CTs for various protection applications, see [1], [2], [7], [10], [13], and [14].

D. Transient Performance of Different CTs With the Same Rating

To illustrate the point discussed in the previous section about trying to make sure that the terminal and neutral-end CTs on a generator differential have the same excitation curve, we can look at two different C800 CTs manufactured to two different designs. Fig. 14 shows two CTs that are both classified as C800 because they each deliver 800 V to a standard burden of 8 Ω at 100 A secondary current. The construction of the two CTs,

though, is different. The CT in Fig. 14a (CT A) is constructed of more copper (R_S is smaller) and less iron (V_E is lower), and the CT in Fig. 14b (CT B) is constructed of more iron (V_E is higher) and less copper (R_S is larger).

If we run each CT through (5) for the same fault condition, we find that the CT in Fig. 14b has a higher chance of saturation—even if the burden loops are exactly the same. Assuming a 2000:5, C800 CT being subjected to a single-line-to-ground fault of 18,000A with an X/R ratio of 25 and an external burden loop of 1.2 Ω, we get the following for the CT in Fig. 14a (smaller R_S):

$$\frac{18,000\,\text{A}}{2,000\,\text{A}} \bullet \frac{1.2\,\Omega + 1\,\Omega}{8\,\Omega + 1\,\Omega} \bullet (25+1) = 57.2 \tag{6}$$

We get the following for the CT in Fig. 14b (larger R_S):

$$\frac{18,000\,\text{A}}{2,000\,\text{A}} \bullet \frac{1.2\,\Omega + 2\,\Omega}{8\,\Omega + 2\,\Omega} \bullet (25+1) = 74.9 \tag{7}$$

Even though the CT in Fig. 14b has more iron (V_E is higher), transiently, (5) predicts that it will saturate more severely.

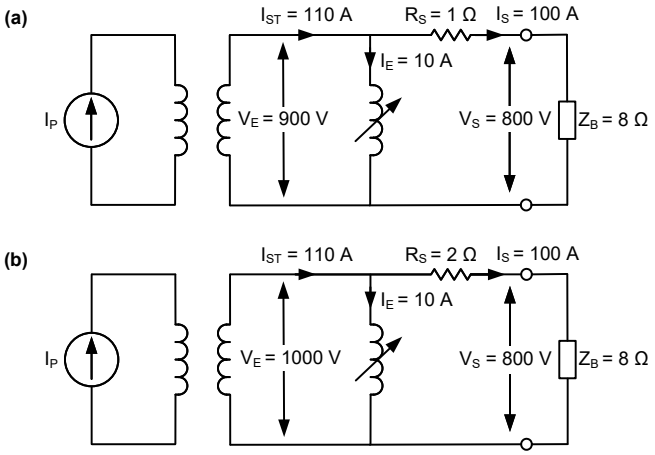

Fig. 14. Two C800 CTs, one with more copper and less iron (a) and one with more iron and less copper (b)

Using a modeling tool like those described in Section III, Subsection E, we can plot the response of both of these CTs and compare the results. Fig. 15 shows the two CTs modeled in a differential circuit, with the differential current being the difference between the two CTs. We can see that the two CTs do indeed perform very similarly except in the second cycle, where CT B saturates sooner than CT A as the evaluation of (5) predicted. After the second cycle, the CTs have nearly the same error and the errors mostly cancel (resulting in little differential current).

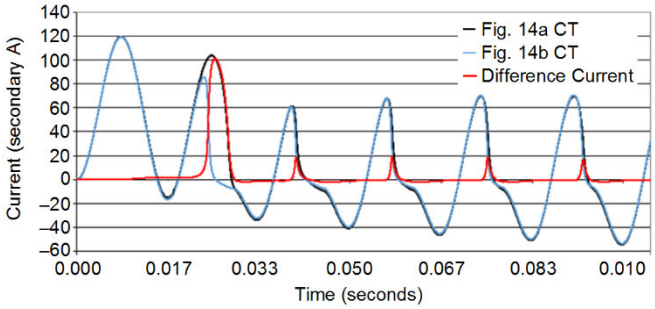

Fig. 15. Transient model of the CTs in Fig. 14

Fig. 16 shows the calculated operate and restraint values for a differential relay connected to these two CTs. We can see that the false differential current reaches over 25 A secondary for almost 1.5 cycles. This relay would have to have a fairly high slope ratio of 40 percent to ride through the transient differential current from these two CTs with the same rating.

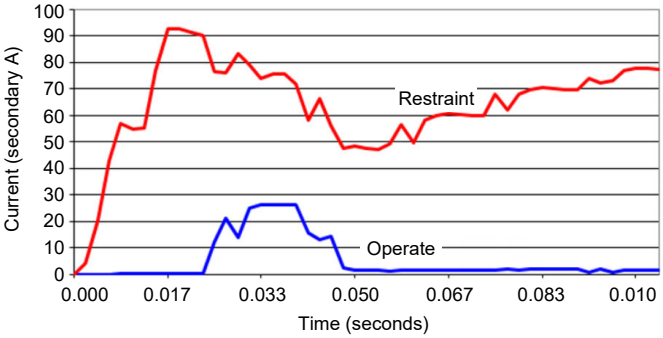

Fig. 16. Operate and restraint values from a differential relay connected to the CTs in Fig. 14

E. CT Analysis Tools

Equation (5) shows how to verify if a CT will saturate for a given fault current and burden. In addition to this equation, other tools exist to analyze the behavior of a CT or sets of CTs.

1) CT Saturation Theory and Calculator

Perhaps the most common is the "CT Saturation Theory and Calculator," an Excel® spreadsheet created by the IEEE Power System Relaying Committee (PSRC) [15]. This spreadsheet is shown in Fig. 17 and is well documented. Using the available tutorials, a level of proficiency can be gained in a short period of time. The necessary inputs are a description of the CT (e.g., ratio, accuracy class, and so on) and data on the available fault current and X/R ratio. The calculator allows the settings and specification engineer to play "what if" scenarios with the CT. Being able to adequately predict the CT's behavior during fault conditions can help form well-reasoned decisions when creating relay settings.

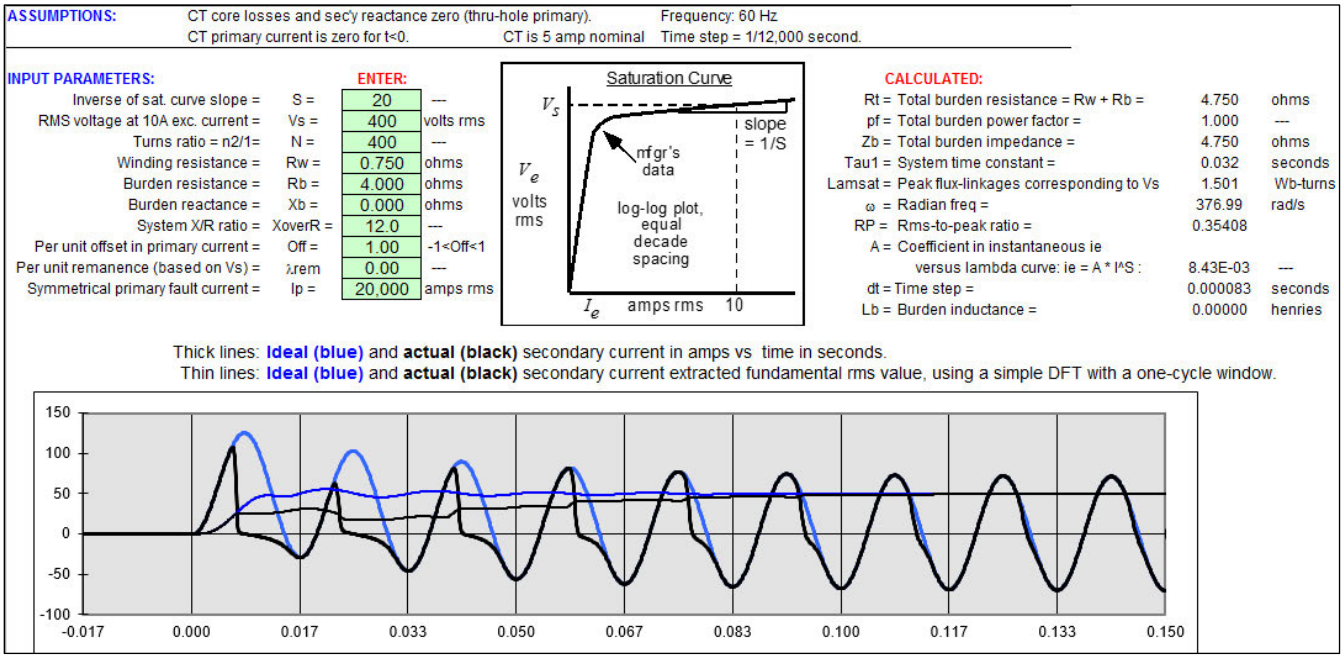

Fig. 17. Simulation in the "CT Saturation Theory and Calculator" spreadsheet for a C400 CT [15]

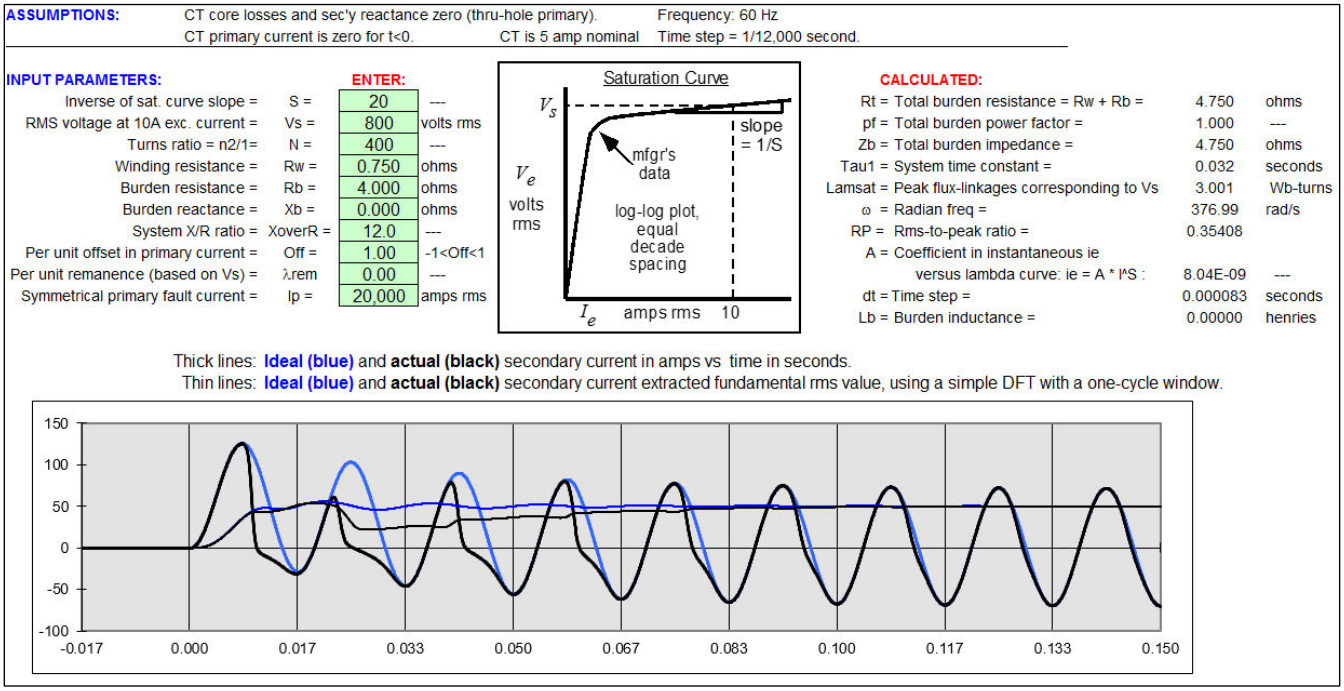

Fig. 18. Simulation in the "CT Saturation Theory and Calculator" spreadsheet for a C800 CT [15]

The simulations in Fig. 17 and Fig. 18 show the difference between a C400 (Fig. 17) and C800 (Fig. 18) CT selection for the same system and burden conditions. If a user runs this simulation for a C400 CT at a certain location, they can easily see that the CT will saturate for the given fault current. At this point, the user has some choices. Because the system fault current and X/R ratio cannot be changed, they can try lowering the burden or using a CT with a higher voltage rating or a higher turns ratio. Fig. 18 shows that a C800 CT will still saturate but less quickly and severely.

2) Two CTs

The authors of [8] developed a program that simulates the transient behavior of two CTs in a differential circuit. The program was originally written in BASIC programming language, but has since been converted to an executable program that can be run on a Windows® operating system (shown in Fig. 19). In addition to plotting the output of the CTs, the program produces ASCII and COMTRADE files that can be used to play the signals into a relay for testing.

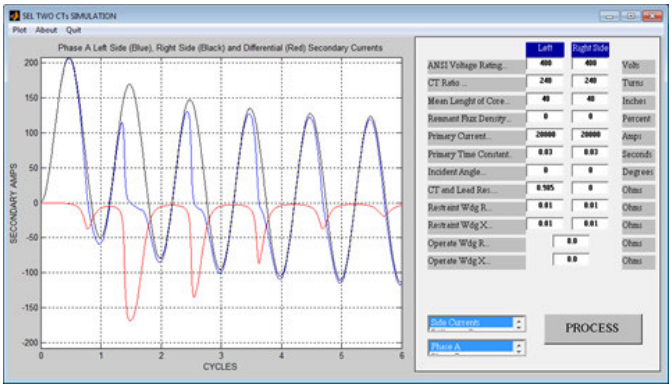

Fig. 19. Two CTs simulation program

In addition to these tools, other software exists to model the transient behavior of CTs—many of which are described in [16].

F. Mitigating Saturation

If any of the analysis in the previous subsections proves that CT saturation is a concern, there are several practical solutions that can be used to mitigate the situation. The most obvious solution is to use a CT with a higher accuracy class, but sometimes these CTs are simply too large physically and do not fit in the given space requirements. Another option is to reduce the CT burden by adding another set of CT cables in parallel. Halving the burden has the same impact on saturation as doubling the accuracy class. Another option is to use CT taps to double the turns ratio. This has an even larger impact—the same as quadrupling the accuracy class. This is because doubling the turns ratio results in halving the secondary current as well as doubling the available voltage at the CT terminals to drive that current through the connected burden. Whenever the turns ratio is increased, ensure that the currents the relay measures during normal operation are still high enough that sensitivity is not lost.

IV. Detecting CT Saturation in Relay Event Reports

Analyzing relay event reports after an operation can be a challenging task, especially when there is doubt about the validity of the operation. Protective relays depend on accurate current and voltage measurements to do their jobs properly. When a CT saturates, the current the relay measures does not represent what is truly on the power system and can cause the relay to behave unexpectedly. The ability to detect when CTs have saturated using relay event reports is necessary to properly analyze relay operation.

A. Raw vs. Filtered Event Reports

Most modern microprocessor-based relays store at least two types of event reports: raw (unfiltered) and filtered. Both event report types are important and are used for different purposes. To understand how to detect CT saturation, we first need to understand the differences between these two report types.

Fig. 20 is a simplified diagram showing how currents are brought into and processed by a microprocessor-based relay. The process for voltages is similar. Current measured by a CT (typically 5 A nominal carried by the CT secondary leads) is brought to the relay inputs and immediately stepped down by an internal transformer to a milliampere-level signal. This current is dropped across a small resistor, resulting in a millivolt-level signal that the relay circuit boards can handle. Next, the voltage is read by an analog-to-digital converter that converts the analog data to digital samples. These samples are then passed through a cosine filter that calculates an equivalent 60 Hz phasor. The goal of this filter is to remove all harmonics outside of the fundamental frequency (60 Hz), as well as any dc offset, to create a 60 Hz signal that can be represented as a phasor with a magnitude and an angle. Most relay algorithms use these phasors (instead of raw samples) to perform their protection functions. For more information on relay filtering, see [17] and [18].

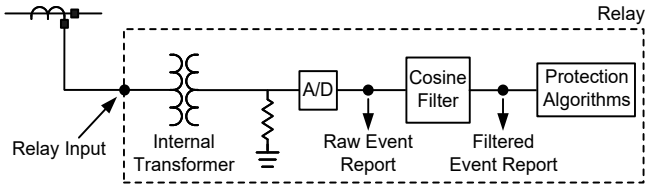

Fig. 20. Simplified signal processing in a microprocessor-based relay

1) Raw Event Reports

Raw event reports are captured before the cosine filter in Fig. 20. Because of this, the data in raw event reports most closely match the actual signals that occur on the power system. The waveforms in these event reports include dc offset and harmonics outside of the fundamental frequency. Current signals in raw event reports are often not as smooth as filtered event reports because the cosine filter has yet to be applied. Event reports downloaded in the COMTRADE file format are always raw data and can be replayed via a test set to a connected relay. Users can change settings and replay an event into their relays to verify correct operation.

2) Filtered Event Reports

Filtered event reports are captured after the cosine filter in Fig. 20. Because relay algorithms also use these quantities, this makes filtered event reports useful in analyzing protective element behavior after a fault. However, because they contain information after the cosine filter, filtered event reports are missing any higher-level harmonics and dc offset, leaving only a 60 Hz waveform that is symmetrical around the zero-axis. This makes it especially difficult to see CT saturation.

An example of the difference between the signals in raw and filtered event reports is shown in Fig. 21. Fig. 21a shows signals from both an unsaturated and a saturated CT in a raw event report. The waveform from the saturated CT (gray line) is very similar to the waveforms in Fig. 5. Fig. 21b shows what this same event looks like in a filtered event report. Notice that the characteristics that make the saturated CT waveform unique are eliminated by the cosine filter, and the resulting signal just looks like normal fault current. As shown in Fig. 21a, most of the signal in the saturated waveform exists at the beginning of each cycle and drops to zero when the CT saturates. Because of this, the resulting phasor (after the cosine filter) will have a reduced magnitude and leading angle compared with what it would be if the CT did not saturate [19].

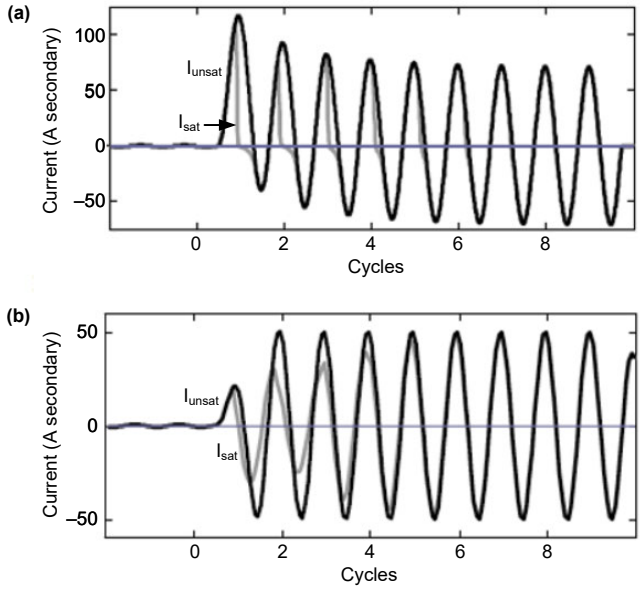

Fig. 21. CT saturation in a raw (a) and filtered (b) event report [19]

3) *Which Type of Event Should I Download?*

Both raw and filtered event types are useful and necessary in event analysis. The type of event report that should be used for analysis depends on whether the protection algorithm being analyzed uses raw or filtered data. The vast majority of protection algorithms use filtered data, and thus the filtered event report is the most often analyzed. However, as shown in Fig. 21, some power system conditions (CT saturation, inrush, and so on) can only be detected in raw event reports because the relay filters remove the characteristics that make them unique. Even the most seasoned event analysis expert will not have much luck looking for CT saturation in filtered event reports. Be sure to understand whether the data is raw or filtered when analyzing a relay operation, and always download both raw and filtered event reports after a fault.

In addition to whether the event report is raw or filtered, it is important to be aware of the sampling rate of the data in the event report. Fig. 22 shows CT saturation error between two CTs that only lasts for a quarter cycle but manages to cause a misoperation [20]. This could easily have been missed if the user was looking at a 4 sample-per-cycle event report. It is important to always download the highest resolution data possible after a fault.

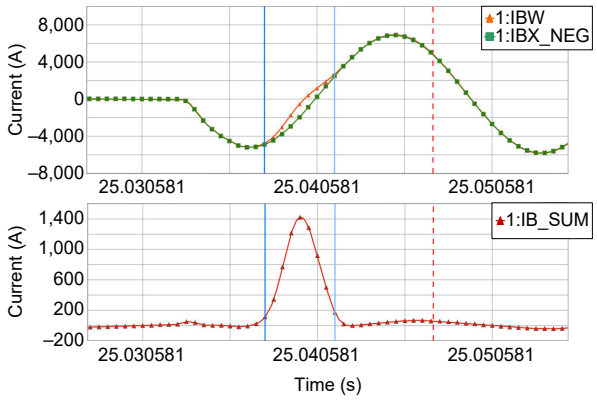

Fig. 22. Difference error from CTs lasting for a quarter cycle

B. *How to Detect Saturation in an Event Report*

To determine if CTs have saturated, relay event reports can be inspected for several known characteristics.

1) *Look for the Characteristic Waveform*

The simplest way to detect CT saturation is to look in the raw event data for the characteristic "sawtooth" current waveforms shown in Fig. 5. Fig. 23 shows a CT that saturated and then recovered during a phase-to-phase fault [21]. This waveform is very similar to the textbook cases, and CT saturation should be immediately suspected.

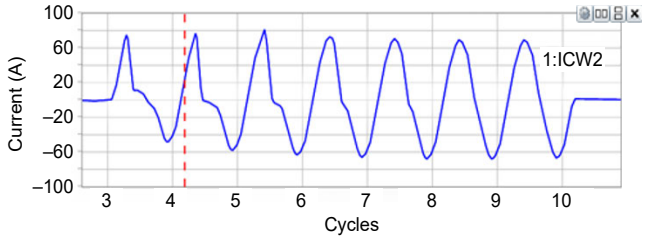

Fig. 23. C-phase CT saturates and recovers during a phase-to-phase fault

Realize that the currents the relay sees will vary depending on what system condition is causing the saturation (fault, inrush, and so on). In general, look for currents to not accurately follow the waveform expected for the given system conditions. Take the system condition of inrush on a power transformer, for example. A relay sees inrush currents when a downstream transformer is first energized, and these inrush currents have an expected signature. Fig. 24 shows three examples of event reports during an inrush condition, each with varying levels of CT saturation. Fig. 24a shows an inrush event with no CT saturation—this is what inrush is supposed to look like [21]. Fig. 24b and Fig. 24c show a different inrush event. In Fig. 24b, the B-phase CT is saturated slightly, and in Fig. 24c, there is severe CT saturation on all three phases.

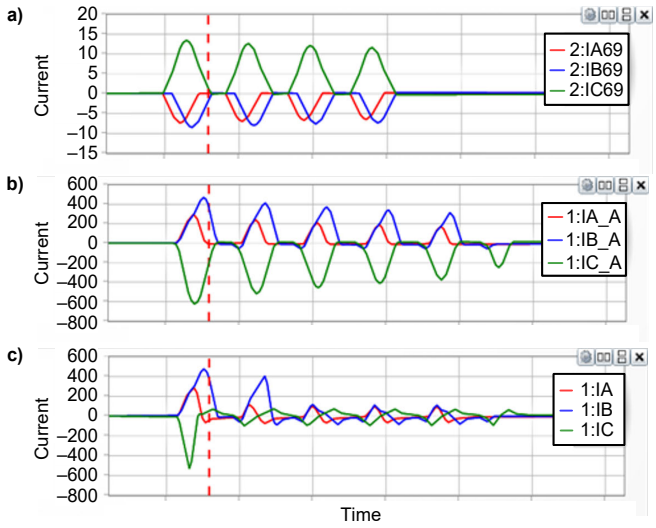

Fig. 24. Inrush currents with no CT saturation (a), slight CT saturation (b), and severe CT saturation (c)

2) Look for Frequency Changes

Depending on the level of CT saturation and how long it persists, it may not always be as obvious as what we have seen so far. Light saturation, while capable of still causing relay misoperations, does not always give us the typical sawtooth waveforms shown previously. Fig. 25 shows a current waveform from a saturated CT that might not be immediately obvious. In cases like this, we can use the fact that saturated CTs output currents rich in harmonics to our advantage. One way to detect higher-level harmonics is to look for frequencies above 60 Hz.

We can detect a change in frequency by using event analysis software to measure and compare the periods of different parts of a signal in a raw event report. In Fig. 25, we placed two vertical lines to create a window that starts at one zero crossing and ends at another zero crossing approximately 1 cycle later. The software shows that the time period between these two lines is 16.147 ms, which is very close to 16.666 ms (1 cycle, based on a 60 Hz nominal frequency). This means that the current signal between these two points in time is almost a true 60 Hz signal and the CT is not experiencing much saturation.

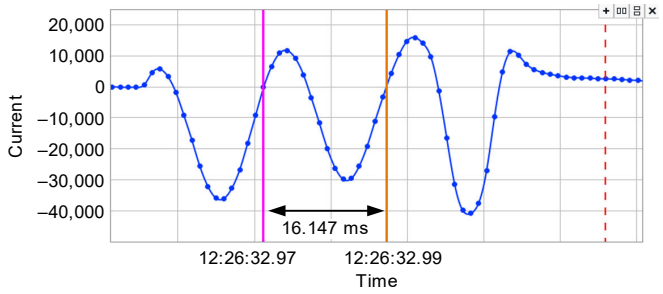

Fig. 25. No frequency distortion exists when the period of a signal is 16.666 ms

Now, we move the time cursors further along the waveform and compare the results. In Fig. 26, the period between the two zero crossings has decreased to 14.616 ms. This shows that the signal has a frequency higher than 60 Hz, and it could be a sign that the CT is saturating.

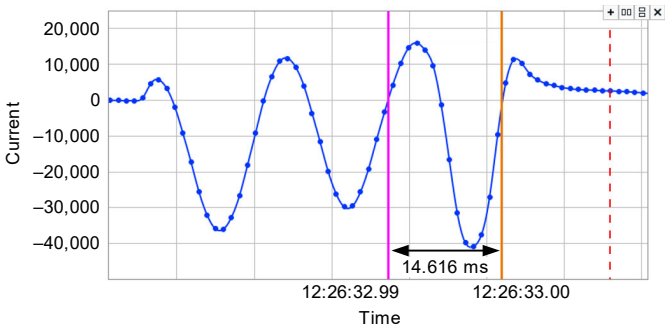

Fig. 26. Frequency is greater than 60 Hz when the period of a signal is less than 16.666 ms

This same technique can be applied to filtered event reports to a certain extent. When a saturated waveform gets passed through the cosine filter, there is some distortion in the output compared with when a nonsaturated waveform gets passed through. For example, the angle of the filtered current phasor will start to go in the leading direction. It is important to note that distortion in a filtered waveform may not be the result of CT saturation—that is just one possible cause. Step changes in magnitude or current reversals from sequential breaker opening (that result in a step change in angle), and evolving faults can cause similar results. However, this distortion is a good hint to download and analyze the raw event report and check for CT saturation.

3) Look for Harmonic Content

Another way to detect if a CT has saturated is to look at the individual harmonics. Asymmetrical saturation produces a large amount of even harmonics and symmetrical saturation produces mainly odd harmonics [22]. Event analysis software can be used to show the amount of harmonic content in the two one-cycle windows of the previous event shown in Fig. 25 and Fig. 26. Fig. 27a shows the second-harmonic content during the first one-cycle window where the CT is not saturating (Fig. 25). Fig. 27b shows the second-harmonic content during the second one-cycle window where the CT is saturating (Fig. 26). Notice that there is significantly more second-harmonic content in the waveform when the CT has saturated.

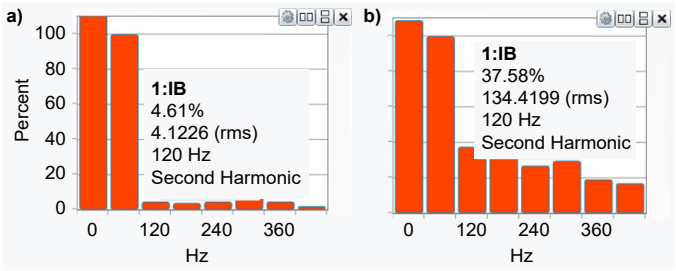

Fig. 27. Second-harmonic content of current waveform when CT is not saturated (a) and is saturated (b)

Just like with frequency changes, CT saturation is not the only cause of harmonic content in current waveforms. The inrush condition shown in the previous section also generates large amounts of harmonic content that the relay will measure. Measuring harmonic content is just one method that can be used when trying to determine if a CT has saturated.

4) Look for a Sudden Loss of DC Offset

In cases where a fault current contains dc offset, the sudden dissipation of this offset can be a sign that CTs have saturated. Theory and testing that shows why dc disappears from the secondary current when saturation occurs is given in [4].

Fig. 28 gives an illustration of what a sudden loss in dc offset looks like. Normally, we would expect a current with dc offset to slowly decay along an exponential curve (shown in red in Fig. 28). We can see that the waveform follows the exponential curve for the first 2–3 cycles, at which point the dc offset completely goes away and the waveform is symmetrical around the 0 axis. If there is rapid dissipation of dc offset in a raw event report, suspect CT saturation.

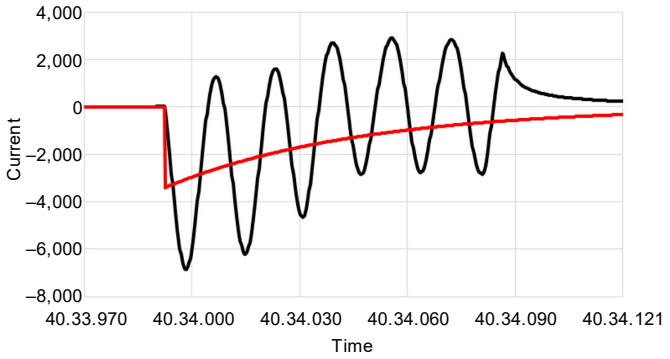

Fig. 28. Example of a sudden loss of dc offset

5) Look for False Residual

False residual current is one sign of CT saturation that can be found in filtered event reports. CT saturation in any of the three phase CTs throws off the balance between the phases and creates false residual ground current. Fig. 29 shows a filtered event report from a delta-wye transformer after an external phase-to-phase fault on a downstream feeder [21]. The top traces (W1) show the phase and residual currents on the wye side of the transformer. CT saturation is suspected because we would not expect zero-sequence current to exist for a phase-to-phase fault. Also notice how the residual current slowly decays with time, which corresponds to the CTs coming out of saturation. The bottom traces (W2) show the phase and residual currents on the delta side of the transformer. We also suspect this to be a false residual current because we would not expect zero-sequence current to exist on the high side of the delta connection for this fault. Note that only unexpected residual current (calculated by the relay as the sum of all three phase CTs or wired into a relay input in a residual connection) is a sign of CT saturation—unexpected neutral current through a core-balanced CT is not. Whenever CT saturation is suspected from filtered event reports, the raw data should be downloaded to verify.

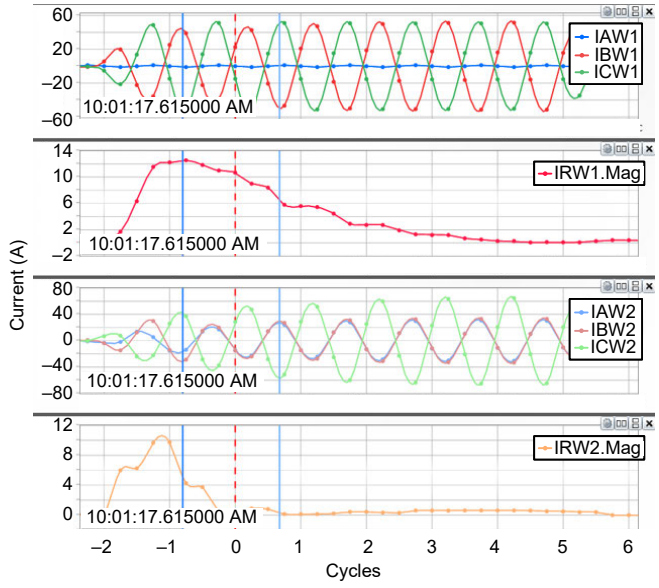

Fig. 29. False residual current appears when CTs saturate during an external fault [21]

6) Differential Applications: Look for Unmatched Currents

Most misoperations of differential applications occur when CTs saturate during external faults. To detect saturation in differential events, we must remember that the differential principle is based on the expectation of the current entering a zone of protection being equal to the current leaving the zone of protection during normal conditions. Fig. 30 shows a raw event report from an external B-phase-to-C-phase fault on a two-terminal differential application. Note the subtle change in IBW1 and ICW1 currents near the 670 ms vertical (orange) time marker. Although the change looks minor, it was enough for this relay to misoperate.

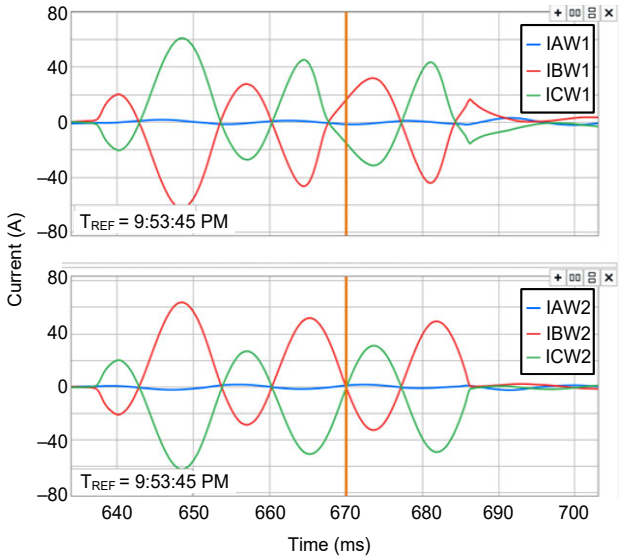

Fig. 30. External B-phase-to-C-phase fault on a two-terminal differential

Based on the principle of differential protection, it is expected that for this external fault, IBW1 will be equal to and 180 degrees out of phase with IBW2. The same is true for ICW1 and ICW2. Fig. 31 shows the B-phase and C-phase currents compared across the differential. The Winding 2 data points are negated to make the difference between waveforms easier to see. If there had been no CT saturation, the curves would be on top of each other. However, we can see that the Winding 1 currents experienced saturation around the 670 ms point in the fault data, causing distortion and a difference from Winding 2. The magnitudes of the differential signals resulting from the saturation on Winding 1 can be found by adding the Winding 1 and Winding 2 data points, as shown by the black traces in Fig. 31.

Whenever phase currents across a differential are not equal and 180 degrees out of phase during an external fault condition, CT saturation is suspected. Remembering to account for CT ratio differences and transformer and CT connections is important, as these things may also result in the phase currents not being equal and 180 degrees out of phase during normal conditions.

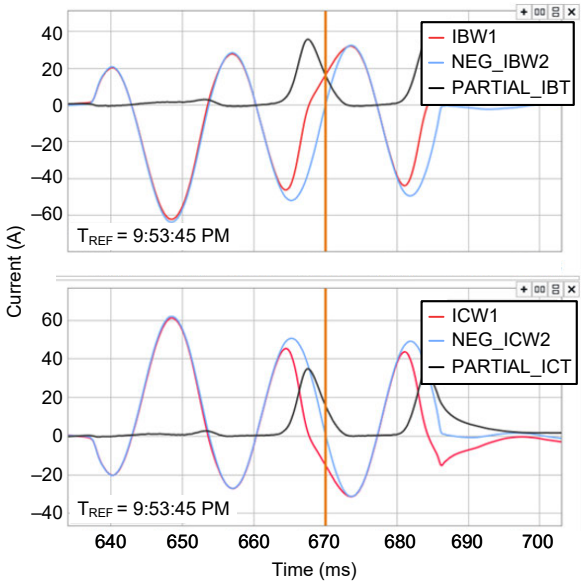

Fig. 31. Comparison of phase CTs with Winding 2 negated

V. Common Misoperations Because of CT Saturation

Section III shows guidelines to follow to reduce the likelihood of saturation occurring in CTs. Despite our best efforts to follow those guidelines, it is inevitable that sometimes CTs saturate and feed unreliable signals to the connected relay. Because relays require undistorted CT secondary current to perform accurate phasor measurements, saturation can lead to misoperations. In other words, "garbage in = garbage out." This section shows two different field cases of CT saturation leading to misoperations in differential installations. In addition to these, there are many other references that document the performance of relay elements during CT saturation, including [1], [5], [7], [10], [19], and [20].

A. Generator Differential Trips During Inrush

A utility feed and a bank of backup generators both feed a switchgear bus. Seven 2,500 kW backup generators are connected to the 13.8 kV generator bus along with a load bank breaker, per Fig. 32. During testing, a 3,500 kVA transformer is connected to the load bank breaker, the breaker is closed into the dead generator bus, and the generators are started. The relay protecting the first generator to close in trips on its differential element.

The differential relays for each backup generator are connected as shown in Fig. 33.

Fig. 34 shows the raw event report that the differential relay recorded. Notice the difference between the bus-side currents and the neutral-side currents. The bus-side currents show a classic, although saturated, inrush waveform (as described previously in Section IV, Subsection B), which makes sense because of the downstream transformer being energized. Section III mentions that we should always match the phase and neutral-side CTs in generator applications to account for the saturation that will inevitably occur. We know the CTs will saturate, but matching the CTs will make sure they saturate in the same way, and the signals will cancel out in the differential.

In this example, because both sets of CTs see the same current with a 180-degree polarity difference, we would expect the same inrush waveform to be mirrored on the neutral side of the generator and the differential to be balanced for this external inrush event. The fact that this is not the case caused the differential element to measure false operate current and trip.

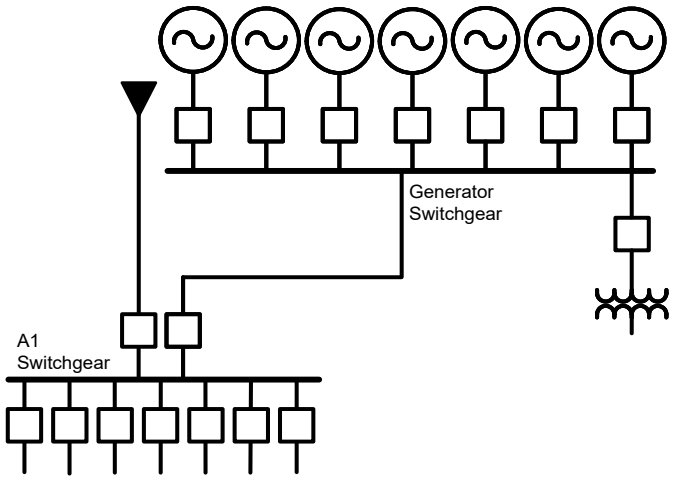

Fig. 32. One-line diagram of utility feed and backup generators

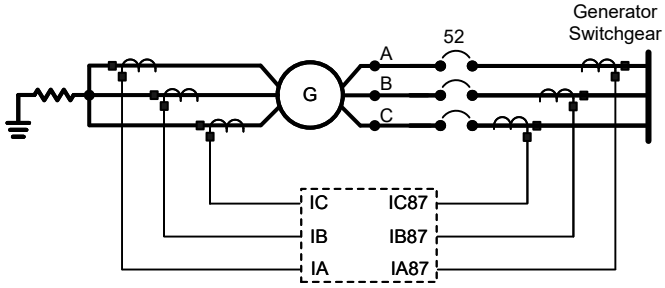

Fig. 33. Connections of differential relays on backup generators

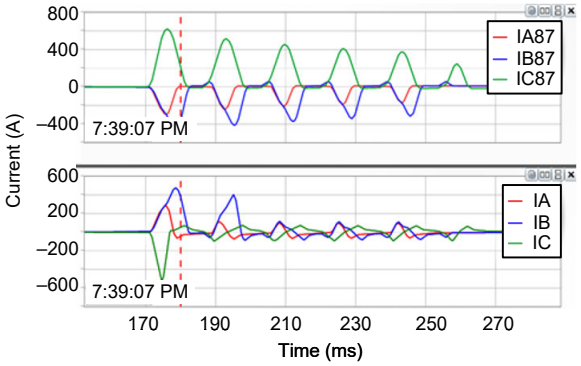

Fig. 34. Raw event report recorded when generator relay trips during startup

Recall from Section II that the presence of asymmetrical fault current can result in CT saturation. This is because of the dc offset in the primary current causing flux to accumulate in one direction more than the other, resulting in the CT eventually hitting its positive or negative volt-time area limit. An inrush waveform (Fig. 34) is harder on CTs than asymmetrical fault current because all of the currents are monopolar. The C-phase current, for instance, only allows accumulation of flux in the positive direction, resulting in hitting the maximum volt-time area much faster than if the current waveform dropped below

zero for some period of time to allow the CT to partially recover.

Fig. 35 shows each phase current from the bus-side CTs compared with its corresponding phase on the neutral side. The bus-side CT signals have been flipped 180 degrees to account for the difference in CT polarity. We can see that the signals start out completely equal to each other (which is expected) and then fall away as the neutral CTs saturate. C-phase is the worst offender, and it is the phase that tripped the relay.

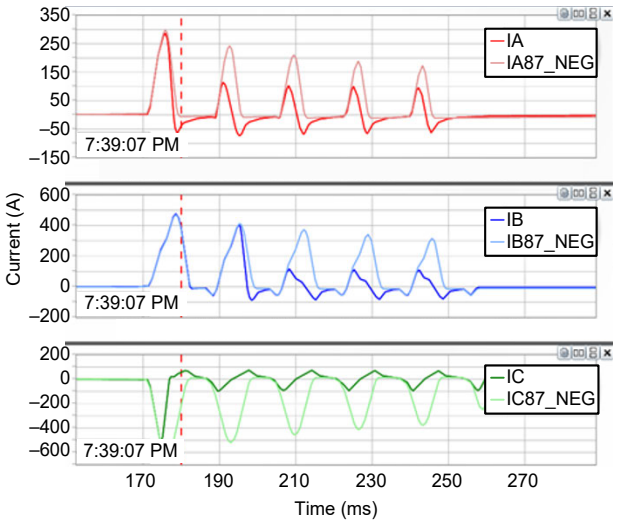

Fig. 35. Currents from bus-side CTs vs. neutral-side CTs

Upon investigation, it was found that the CTs in fact were sized the same on both sides of the generator—both 200/5, C20, intentionally sized to the generator's full-load ampere rating of 150 A. With CTs rated similarly, it is unlikely that one set would perform so differently than the other. It was then found that the length of the CT secondary leads between the CTs and the relay were considerably different. The one-way lead length of the bus-side CTs was 15 feet, while the neutral-side CTs were 20 times longer—300 feet! This greatly increased the burden of the neutral-side CTs (2.44 Ω for the neutral side vs. 0.17 Ω for the bus side) and resulted in the difference in saturation behavior.

The ideal solution to this problem is to match the lead length burden on both sets of CTs to where they saturate similarly and balance each other out. Until that could be accomplished, a temporary measure was taken by forcing the relay into high security mode for a short time during startup, when the generator breaker first closed. High security mode was then programmed to have a higher minimum operate current and a more secure slope setting than the standard settings.

B. Transformer Relay Operates During DC Offset

In March of 2017, a transformer differential relay misoperated on an external A-phase-to-ground fault on the low side of a 138/69 kV wye-wye autotransformer. The filtered event report from this operation is shown in Fig. 36. The relay and CTs are configured such that the taps on both sides are equal, and thus we would expect the A-phase currents on Winding 1 and Winding 2 to be equal and 180 degrees out of phase with each other. We can tell from the waveforms on the bottom of Fig. 36 that this is not the case. We would also expect the nonfaulted phases to remain balanced, with 120-degree separation—but, Fig. 36 shows that this is also not the case. We can suspect CT saturation, but we will not know for sure until we look at the raw signals.

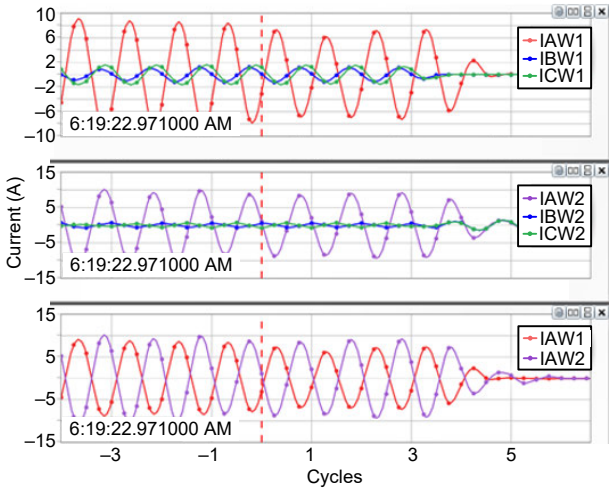

Fig. 36. Filtered event report for external A-phase-to-ground fault

Fig. 37 shows the filtered differential event report. Here, we see the restraint currents steadily decreasing throughout the event, while operate currents increase and then decrease. Decreasing operate current over time, while filtered phase currents remain steady throughout a fault, is an indication of CT saturation [21].

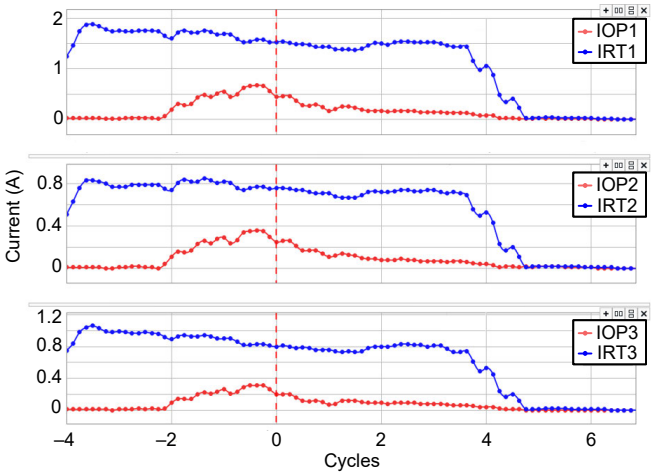

Fig. 37. Filtered differential event shows decreasing operate current over time

Fig. 38 shows the raw event report. Here we can see that the A-phase currents on Winding 1 and Winding 2 have a significant amount of dc offset at the beginning of the fault. After about seven cycles, the dc offset goes away and the waveforms balance out. Note that this dc offset cannot be seen in the filtered event report because it is removed by the cosine filter. The dc offset itself does not cause the misoperation, but it does cause the CTs to saturate. The bottom graph in Fig. 38 shows the A-phase current on Winding 1 compared with the inverse of the A-phase current on Winding 2, and it proves that these signals are not equal and 180 degrees out of phase because

the CTs have saturated. Notice that the period of the event that has the most difference between the current signals in Fig. 38 corresponds to the period in the event with the highest operate current in Fig. 37. It is this difference in CT behavior that causes false operate current and results in the relay tripping on its differential element. A very similar event is shown in [21]—an external phase-to-ground fault on the wye side of a delta-wye transformer with significant dc offset.

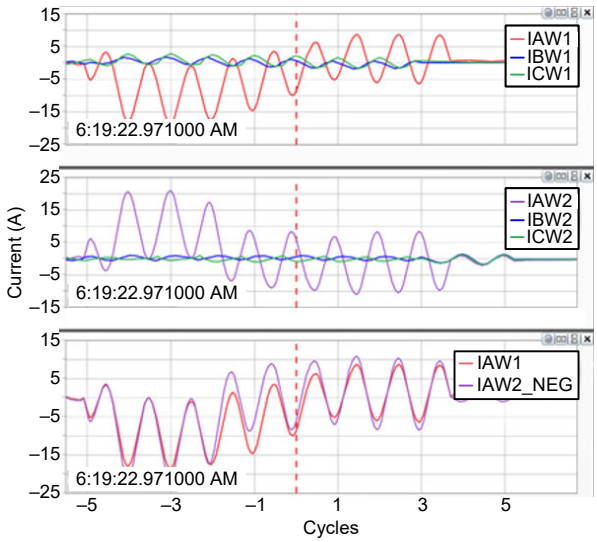

Fig. 38. Raw event report shows significant dc offset

Several solutions could be implemented to prevent this type of misoperation. In this case, the utility chose to temporarily raise the minimum operate current threshold and slope setting in the differential relay. At a later date, they plan to increase the taps of the CTs to allow for a higher voltage before saturation (from 300/5 to 800/5 on the 138 kV side, and from 600/5 to 1200/5 on the 69 kV side) and return the slope to its previous setting. The external fault detection algorithm described in the next section would also have prevented this misoperation because restraint current increased in all three phases significantly before the operate current increased. This would have put the relay into a more secure mode with a higher slope setting and kept it there until the dc offset decayed.

VI. Relay Algorithms Account for Saturation

Even with comprehensive analysis and our best intentions, it is often difficult or impossible to avoid saturation for a given system. In these instances, relay algorithms may be able to assist by either desensitizing or delaying operation during CT saturation.

A. Percentage-Restrained Differential

A percentage-restrained differential relay works off the principle that the current going into a zone of protection must equal the current leaving the zone under balanced conditions. This can be implemented by calculating an operate and restraint quantity using (8).

$$I_{OP} = \left|\vec{I1} + \vec{I2}\right|$$
$$I_{RT} = \left|\vec{I1}\right| + \left|\vec{I2}\right| \quad (8)$$

Because the CTs around the zone are assumed to have opposing polarities, the operate quantity (I_{OP}) calculates as the difference between the current into and out of the zone. Under normal load or through-fault conditions, I_{OP} should equal 0, and under internal fault conditions, I_{OP} calculates to a value. However, if one of the CTs enclosing the zone saturates during an external fault, the currents from the CTs no longer cancel each other out exactly, and I_{OP} calculates to some value. We do not want to trip for this condition, so we must add a margin to provide security for CT errors. This is normally done by comparing I_{OP} with I_{RT} times a slope (see (9))—instead of comparing it with a fixed value—which can be set to an appropriate margin to account for CT saturation errors. This works well because when currents are high (high values of I_{RT}) and the chance for saturation is greater, I_{OP} needs to overcome a larger threshold before the relay trips. Similar to the slope in percentage-restrained differential relays, the angle of the characteristic of an alpha-plane differential relay also helps account for CT saturation differences between the two sets of CTs.

$$I_{OP} \geq SLP \bullet I_{RT} \quad (9)$$

B. External Fault Detector Enables High Security Mode

When an external fault occurs and causes the CTs to saturate, there is a small window of time when the fault first occurs that the CTs have not yet saturated. During this time period, I_{RT} increases because of the elevated fault current, but I_{OP} does not. We can use this to our advantage to develop logic that detects an external fault before the CTs have had a chance to saturate. When the relay detects a large change in I_{RT} with no (or very small) change in I_{OP}, it declares an external fault. This is shown in Fig. 39. The success of this logic depends on CTs providing valid output for some amount of time (2 ms to a half cycle) [14] [20].

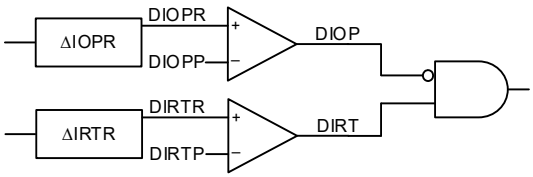

Fig. 39. External fault detection logic

Using this logic, a relay can automatically desensitize itself to an external fault (when CT saturation is likely to occur). Although not every external fault will result in saturated CTs, it is best to default to a higher security (less sensitive) protective mode for a short period of time. This higher security mode can include a higher slope value and/or a higher minimum operate current required to operate the differential element. Some relays use the second-harmonic content present in the waveforms of saturated CTs to extend the time the differential element is in high security mode [14].

C. Cosine-Peak Adaptive Filtering

In switchgear applications, CTs are notoriously undersized, primarily because of space restrictions. Higher accuracy classes require more turns or more iron and result in physically larger CTs. Even when it is known that a higher accuracy class is needed, there is simply not room for these larger CTs in many switchgear lineups. In addition, switchgear is serving loads in some of the highest magnitude fault current locations in the power system. This combination yields fault currents that can exceed 200 times the CT primary current rating and all but assures that saturation will regularly occur. Overcurrent elements are used very frequently in these applications, so it is important that they function correctly, even during saturation.

Section IV shows that current magnitudes and angles are calculated from analog data using a cosine filter. This cosine filter is excellent at removing dc offset and harmonics, but it is slow to provide the correct magnitude when CTs are saturated. A slow filter output results in overcurrent elements taking longer to operate for a fault because the reported current magnitude stays below the pickup threshold for a longer time. Another type of filter, the bipolar peak detector, provides a better estimation of the current magnitude during CT saturation. The response of these two filters to a saturated signal from a CT is shown in Fig. 40, along with an instantaneous overcurrent pickup setting of 80 A secondary.

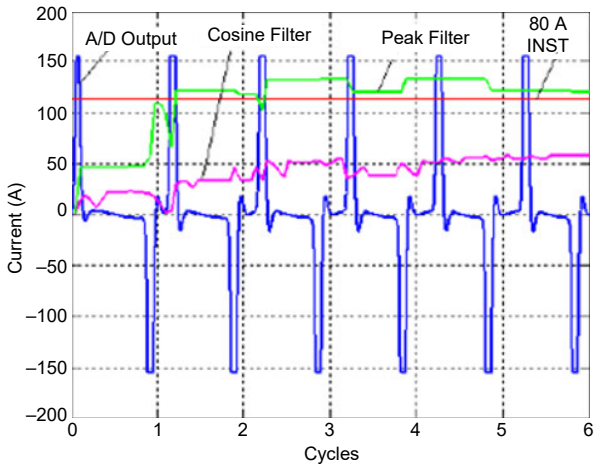

Fig. 40. Response of cosine filter and peak detector filter to a saturated waveform [23]

When an instantaneous overcurrent element is set with a pickup of 40 A secondary or higher, modern relay algorithms can use harmonic content to detect when CTs are saturating and switch between the cosine and bipolar peak detector filters accordingly. This results in secure performance at lower fault currents and faster performance during CT saturation. For more information on the bipolar peak detector filter, see [23], [24], and [25].

Although modern relay algorithms can help accommodate some level of CT saturation, these algorithms are not an excuse to bypass the calculations in Section III or use underrated CTs. If saturation is expected and the relay algorithms are depended upon to account for it, it is always best to simulate the fault using a transient program to validate how the relay responds.

VII. Conclusion

The following are important takeaways from this paper:

- A CT works by the principle of electromagnetic induction. Current flowing in the primary winding of a CT generates an alternating magnetic flux, which in turn induces an alternating voltage across the secondary winding.
- The iron core of a CT is made up of a fixed number of molecular magnets, which line up dynamically with the alternating magnetic field. When all the magnets are aligned in the same direction, the maximum flux density is reached and the CT core is said to be saturated.
- There are two types of CT saturation: symmetrical saturation and asymmetrical saturation. Symmetrical saturation is caused by symmetrical fault currents high in magnitude, while asymmetrical saturation is caused by fault currents with dc offset.
- When a breaker trips during asymmetrical current (before the dc component dissipates), remanence can remain in the CT core and affect its behavior when it is next energized.
- A simple CT equivalent circuit can be used to model CT behavior using rms quantities.
- The knee point of a CT excitation graph is not the same thing as the saturation voltage. The accuracy class voltage rating of the CT is a better estimate of the saturation voltage.
- IEEE defines the voltage rating as the CT secondary voltage that the CT delivers when it is connected to a standard secondary burden at 20 times rated secondary current without exceeding a 10 percent ratio error [2].
- The voltage rating for a CT is only valid for its full ratio and changes if the CT is tapped down.
- Equation (5) can be used to determine the maximum allowable fault current for a given burden, or maximum allowable burden for a given fault current, while avoiding saturation.
- It is important to understand the difference between raw and filtered event reports and to download both types of data (at the highest sampling rate available) from relays after a fault.
- CT saturation can be detected in raw event reports by looking for the characteristic waveform, frequency changes, or harmonic content. Filtered event reports can be inspected for false residual current.
- Saturated CTs feed incorrect signals to relays and can result in relay misoperations, mainly in differential applications.
- Although many existing protection algorithms account for some degree of CT saturation, this does not excuse the engineer from performing due diligence in selecting appropriate CTs for the application.

VIII. Appendix A

To meet the IEEE C57.13-1993 standard, a CT must not exceed 10 percent ratio correction (PRC) [26]. The standard defines the following:

- The ratio correction factor (RCF) is the ratio of the true ratio to the marked ratio. The primary current is equal to the secondary current multiplied by the marked ratio times the RCF.
- The percent ratio correction (PRC) is the difference between the RCF and unity, expressed in percent.

We can write the definition of RCF as shown in (10), where CTR is the marked ratio of the CT.

$$\begin{aligned} \text{RCF} &= \frac{I_P / I_S}{\text{CTR}} \\ \text{RCF} &= \frac{I_{ST}}{I_S} \end{aligned} \tag{10}$$

We can write the definition of PRC as shown in (11).

$$\text{PRC} = (\text{RCF} - 1) \bullet 100 \tag{11}$$

Substituting (10) into (11), we get (12).

$$\begin{aligned} \text{PRC} &= \left(\frac{I_{ST}}{I_S} - 1 \right) \bullet 100 \\ \text{PRC} &= \left(\frac{I_{ST}}{I_S} - \frac{I_S}{I_S} \right) \bullet 100 \\ \text{PRC} &= \left(\frac{I_{ST} - I_S}{I_S} \right) \bullet 100 \\ \text{PRC} &= \frac{I_E}{I_S} \bullet 100 \end{aligned} \tag{12}$$

IEEE C57.13-1993 states that (12) must not exceed 10 percent [26]. We want to know what this limit means in terms of how the actual secondary current corresponds to the expected, or ideal, secondary current. A more intuitive form of calculating CT error would be $\frac{I_{S\_actual}}{I_{S\_expected}}$, or $\frac{I_S}{I_{ST}}$. We can write this as shown in (13).

$$\frac{I_S}{I_{ST}} = \frac{I_S}{I_S + I_E} \tag{13}$$

If we divide all terms on the right side by I_S, we get (14).

$$\frac{I_S}{I_{ST}} = \frac{1}{1 + \frac{I_E}{I_S}} \tag{14}$$

Since $\frac{I_E}{I_S} \le 10$ percent, we get (15).

$$\frac{I_S}{I_{ST}} \ge 0.909 \tag{15}$$

Therefore, the actual secondary current coming out of the CT must be greater than or equal to 90 percent of what we expect it to be. This means that only 10 percent of the expected signal can be lost as error.

IEEE C57.13-2016 states that CTs must have ≤10% *ratio error* to meet the standard [9]. Ratio error is defined similarly to PRC in IEEE C57.13-1993, but with an added sine term to account for the fact that I_E and I_S are not exactly in phase for cases when the connected burden has a resistive component. When the connected burden is not purely inductive, I_E and I_S cannot simply be added algebraically, and this extra term is needed for accuracy.

IEEE C57.13-2016 also defines the *composite error* the same way IEEE C57.13-1993 defines PRC, and it says that this can be used in place of ratio error for ring-type cores of low reactance. For more on CT measurement errors, see [27].

For simplicity in this paper, we define ratio error the same as PRC, as shown in (16).

$$\text{Ratio Error (\%)} = \frac{I_E}{I_S} \bullet 100 \tag{16}$$

IX. Appendix B

Recall from Section II that the ANSI voltage rating of a CT defines the minimum secondary voltage (V_S) that the CT must deliver to a standard burden at 20 times rated secondary current without exceeding a 10 percent ratio error [2]. If the fault current through a CT is higher than 20 times the rated current, or the connected burden is higher than the standard burden, we may risk going into saturation (over 10 percent error). We can use the definition for the ANSI standard voltage rating to develop an equation for the level of fault current (or connected burden) that, if we go above, will result in more than 10 percent error. We can call this the saturation point for symmetrical current (symmetrical saturation).

We can write the definition of the ANSI standard voltage rating as follows:

$$V_{STD} = 20 \bullet I_{S\,RATED} \bullet Z_{B\,STD} \tag{17}$$

where:

V_{STD} is the secondary terminal voltage rating

$I_{S\,RATED}$ is the rated secondary current

$Z_{B\,STD}$ is the standard burden

Fig. 41 is a reproduction of Fig. 8, for convenience.

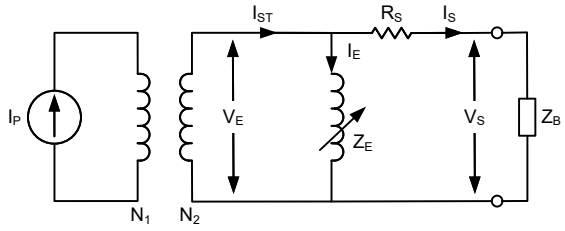

Fig. 41. Simplified CT equivalent circuit

Using the equivalent circuit in Fig. 41 and the definition of the ANSI voltage rating, we know that the ratio error will not exceed 10 percent as long as the secondary terminal voltage V_S is less than the secondary terminal voltage rating V_{STD}, as shown in (18).

$$V_S \le V_{STD} \tag{18}$$

The voltages V_S and V_{STD} are driven by the core excitation voltage, V_E. Therefore, we can also write the relationship in (18) as (19), which considers the voltage drop across the secondary winding resistance R_S.

$$V_E \le V_{E\,STD} \tag{19}$$

We can write the definition of $V_{E\,STD}$ as:

$$V_{E\,STD} = 20 \bullet I_{S\,RATED} \bullet \left(Z_{B\,STD} + R_S\right) \tag{20}$$

We can write the actual voltage V_E as:

$$V_E = I_S \bullet \left(Z_B + R_S\right) \tag{21}$$

Therefore, based on the relationship in (19):

$$I_S \bullet \left(Z_B + R_S\right) \le 20 \bullet I_{S\,RATED} \bullet \left(Z_{B\,STD} + R_S\right) \tag{22}$$

Rearranging terms, we obtain:

$$\frac{I_S}{I_{S\,RATED}} \bullet \frac{Z_B + R_S}{Z_{B\,STD} + R_S} \le 20 \tag{23}$$

To make this equation useful, we must write it in terms of the secondary fault current, which is I_{ST} in Fig. 41. I_{ST} is the sum of I_S and I_E. For the worst case right at the saturation point, [9] defines the error as 10 percent ($I_E/I_S \le 0.1$). Using this relationship, we can define:

$$I_S = 0.909 \bullet I_{ST} \tag{24}$$

We can then write (23) as:

$$\frac{0.909 \bullet I_{ST}}{I_{S\,RATED}} \bullet \frac{Z_B + R_S}{Z_{B\,STD} + R_S} \le 20 \tag{25}$$

If we define I_{ST} as the secondary fault current $I_{f\,sec}$, (25) becomes:

$$\frac{I_{f\,sec}}{I_{S\,RATED}} \bullet \frac{Z_B + R_S}{Z_{B\,STD} + R_S} \le 22 \tag{26}$$

We can use (26) to solve for the maximum fault current ($I_{f\,sec}$) that the CT can handle before it goes into saturation. We can also use it to solve for the maximum burden for a given fault current.

In development of (26), we assumed an inductive burden. Therefore, I_S and I_E are in phase and can be added algebraically to get I_{ST}. This assumption also allows us to use the simplified error equation for ratio error in Appendix A. Using modern resistive burdens with these simplified equations produces errors. To account for these errors, a more conservative form of (19) is used:

$$\frac{I_{f\,sec}}{I_{S\,RATED}} \bullet \frac{Z_B + R_S}{Z_{B\,STD} + R_S} \le 20 \tag{27}$$

Because we are concerned with primary fault current values, we can incorporate the CT ratio and convert the first term in (27) to primary values. This results in (28).

$$\frac{I_{FAULT}}{I_{PRI}} \bullet \frac{Z_B + R_S}{Z_{B\,STD} + R_S} \le 20 \tag{28}$$

where:

I_{FAULT} is the maximum fault current in primary amperes for a given fault.

I_{PRI} is the primary current rating of the CT (e.g., for a 2000/5 CT, I_{PRI} is 2000.)

Z_B is the actual burden of the CT's secondary circuit, which includes both the impedance of the connected relay and the impedance of the leads from the CT to the relay.

R_S is the internal resistance of the CT secondary winding.

$Z_{B\,STD}$ is the standard burden of the CT (e.g., for a C800 CT, the $Z_{B\,STD}$ is 8 Ω.)

Equation (28) can be used to evaluate CT performance for symmetrical fault currents but should never be used in practice. This derivation of (28) is shown simply as a basis for (5). Equation (28) is not adequate for analyzing how a CT will behave in the presence of (typically asymmetrical) fault current, and (5) should always be used in practice. For even better accuracy, use a transient modeling program to model CT behavior in the time domain.

Note that the basis for (28) was first introduced in [1]. Later, in [5], the original equation was adjusted to consider the CT secondary resistance R_S, resulting in the more accurate analysis reflected here.

X. Appendix C

Equation (5), repeated in (29), is used to analyze CT saturation resulting from fault current with dc offset.

A C800, 2000/5 CT with $R_S = 0.5\ \Omega$ is connected to a 1 Ω burden (including relay and lead resistance). The system X/R ratio is 12. What is the maximum primary three-phase fault current that can be applied to this CT without exceeding the maximum flux density (which is proportional to the volt-time area)?

To determine the maximum fault current, set (5) to the maximum of 20 and solve for I_{FAULT}, as shown in (29) and (30).

$$\frac{I_{FAULT}}{I_{PRI}} \bullet \frac{Z_B + R_S}{Z_{B\,STD} + R_S}\left(\frac{X}{R} + 1\right) \le 20 \tag{29}$$

$$\frac{I_{FAULT}}{2000} \bullet \frac{1\ \Omega + 0.5\ \Omega}{8\ \Omega + 0.5\ \Omega}(12 + 1) \le 20$$

$$I_{FAULT} = 17.4\ \text{kA} \tag{30}$$

XI. References

[1] S. E. Zocholl, *Analyzing and Applying Current Transformers*. Schweitzer Engineering Laboratories, Inc., Pullman, WA, 2004.

[2] IEEE Standard C37.110-2007, IEEE Guide for the Application of Current Transformers Used for Protective Relaying Purposes.

[3] D. Subedi and S. Pradhan, "Analyzing Current Transformers Saturation Characteristics for Different Connected Burden Using LabVIEW Data Acquisition Tool," *International Journal of Electrical, Computer, Energetic, Electronic and Communication Engineering*, Vol. 9, Issue 10, 2015.

[4] B. Kasztenny, N. Fischer, D. Taylor, T. Prakash, and J. Jalli, "Do CTs like DC? Performance of Current Transformers With Geomagnetically Induced Currents," proceedings of the 69th Annual Conference for Protective Relay Engineers, College Station, TX, April 2016.

[5] M. Thompson and R. Folkers, "Secure Application of Transformer Differential Relays for Bus Protection," proceedings of the 58th Annual Conference for Protective Relay Engineers, College Station, TX, April 2005.

[6] S. Hodder, B. Kasztenny, N. Fischer, and Y. Xia, "Low Second-Harmonic Content in Transformer Inrush Currents – Analysis and Practical Solutions for Protection Security," proceedings of the 67th Annual Conference for Protective Relay Engineers, College Station, TX, March 2014.

[7] H. J. Altuve, N. Fischer, G. Benmouyal, and D. Finney, "Sizing Current Transformers for Line Protection Applications," proceedings of the 66th Annual Conference for Protective Relay Engineers, College Station, TX, April 2013.

[8] S. E. Zocholl and D. W. Smaha, "Current Transformer Concepts," proceedings of the 46th Annual Georgia Tech Protective Relaying Conference, Atlanta, GA, April 1992.

[9] IEEE Standard C57.13-2016, IEEE Standard Requirements for Instrument Transformers.

[10] G. Benmouyal, J. Roberts, and S. E. Zocholl, "Selecting CTs to Optimize Relay Performance," proceedings of the Pennsylvania Electric Association Relay Committee Fall Meeting," September 1996.

[11] S. Manson and A. Upreti, "Current Transformer Selection Techniques for Low-Voltage Motor Control Centers," proceedings of the 63rd Annual Petroleum and Chemical Industry Technical Conference, Philadelphia, PA, September 2016.

[12] J. R. Linders, C. W. Barnett, J. W. Chadwick, P. R. Drum, K. J. Khunkhun, W. C. Kotheimer, P. A. Kotos, D. W. Smaha, J. W. Walton, P. B. Winston, and S. E. Zocholl, "Relay Performance Considerations With Low-Ratio CTs and High-Fault Currents," *IEEE Transactions on Industry Applications*, Vol. 31, Issue 2, March–April 1995.

[13] S. E. Zocholl, "Rating CTs for Low Impedance Bus and Machine Differential Applications," proceedings of the 27th Annual Western Protective Relay Conference," Spokane, WA, October 2000.

[14] M. Donolo, A. Guzmán, M. V. Mynam, R. Jain, and D. Finney, "Generator Protection Overcomes Current Transformer Limitations," proceedings of the 41st Annual Western Protective Relay Conference, Spokane, WA, October 2014.

[15] IEEE Power System Relaying and Control Committee, "CT Saturation Theory and Calculator." Available: http://www.pes-psrc.org.

[16] R. Folkers, "Determine Current Transformer Suitability Using EMTP Models," proceedings of the 26th Annual Western Protective Relay Conference, Spokane, WA, October 1999.

[17] E. O. Schweitzer, III and D. Hou, "Filtering for Protective Relays," proceedings of the 19th Annual Western Protective Relay Conference, Spokane, WA, October 1992.

[18] S. E. Zocholl and G. Benmouyal, "How Microprocessor Relays Respond to Harmonics, Saturation, and Other Wave Distortions," proceedings of the 24th Annual Western Protective Relay Conference, Spokane, WA, October 1997.

[19] J. Mooney, "Distance Element Performance Under Conditions of CT Saturation," proceedings of the 61st Annual Conference for Protective Relay Engineers, College Station, TX, April 2008.

[20] D. Costello, J. Young, and J. Traphoner, "Paralleling CTs for Line Current Differential Applications: Problems and Solutions," proceedings of the 68th Annual Conference for Protective Relay Engineers, College Station, TX, March–April 2015.

[21] D. Costello, "Lessons Learned Through Commissioning and Analyzing Data From Transformer Differential Installations," proceedings of the 60th Annual Conference for Protective Relay Engineers, College Station, TX, March 2007.

[22] L. F. Kennedy and C. D. Hayward, "Harmonic-Current-Restrained Relays for Differential Protection," *Electrical Engineering*, Vol. 57, Issue 5, May 1938, pp. 262–271.

[23] L. Underwood, "Current Transformer Selection Criteria for Relays with Adaptive Overcurrent Elements," April 2005. Available: selinc.com.

[24] S. E. Zocholl and J. Mooney, "Primary High-Current Testing of Relays With Low Ratio Current Transformers," proceedings of the 57th Annual Conference for Protective Relay Engineers, College Station, TX, April 2004.

[25] G. Benmouyal and S. E. Zocholl, "The Impact of High Fault Current and CT Rating Limits on Overcurrent Protection," proceedings of the 56th Annual Conference for Protective Relay Engineers, College Station, TX, April 2003.

[26] IEEE Standard C57.13-1993, IEEE Standard Requirements for Instrument Transformers.

[27] Forest K. Harris, *Electrical Measurements*. John Wiley & Sons, Hoboken, NJ, 1952.

XII. BIOGRAPHIES

Ariana Hargrave earned her B.S.E.E., magna cum laude, from St. Mary's University in San Antonio, Texas, in 2007. She graduated with a Master's of Engineering in electrical engineering from Texas A&M University in 2009, specializing in power systems. Ariana joined Schweitzer Engineering Laboratories, Inc. in 2009 and works as a protection application engineer in Fair Oaks Ranch, Texas. She is an IEEE member and a registered professional engineer in the state of Texas.

Michael J. Thompson received his B.S., magna cum laude, from Bradley University in 1981 and an M.B.A. from Eastern Illinois University in 1991. Upon graduating, he served nearly 15 years at Central Illinois Public Service (now AMEREN). Prior to joining Schweitzer Engineering Laboratories, Inc. (SEL) in 2001, he was involved in the development of several numerical protective relays while working at Basler Electric. He is presently a Fellow Engineer at SEL Engineering Services, Inc. He is a senior member of the IEEE, member of the IEEE PES Power System Relaying and Control Committee, past chairman of the Substation Protection Subcommittee of the PSRCC, and received the Standards Medallion from the IEEE Standards Association in 2016. Michael is a registered professional engineer in six jurisdictions, was a contributor to the reference book "Modern Solutions for the Protection Control and Monitoring of Electric Power Systems," has published numerous technical papers and magazine articles, and holds three patents associated with power system protection and control.

Brad Heilman, P.E., has a B.S.E.E. degree from the South Dakota School of Mines and Technology. From 1990 to 1997, he was employed as a system protection engineer for Black Hills Power & Light. His utility work included transmission line and generator protection, power plant and substation commissioning, and SCADA system upgrades. In 1997, he joined Schweitzer Engineering Laboratories, Inc. as a field application engineer supporting customers in Arizona, California, Montana, Wyoming, Utah, North Dakota, Nebraska, Nevada, Idaho, and South Dakota. He is an IEEE member and licensed professional engineer in the state of South Dakota.

Previously presented at the 2018 Texas A&M Conference for Protective Relay Engineers.

20200501 • TP6811-01